JOC The Journal of Organic Chemistry

Article

pubs.acs.org/joc

Solid-Phase Synthesis of Water-Soluble Helically Folded Hybrid α-Amino Acid/Quinoline Oligoamides

Xiaobo Hu,[†] Simon J. Dawson,[‡] Yui Nagaoka,[§] Aya Tanatani,[§] and Ivan Huc*[,†]

[†]Université de Bordeaux, CBMN (UMR5248), Institut Européen de Chimie et Biologie, 2 Rue Escarpit, 33600 Pessac, France

[‡]CNRS, CBMN (UMR 5248), Institut Européen de Chimie et Biologie, 2 Rue Escarpit, 33600 Pessac, France

[§]Department of Chemistry, Faculty of Science, Ochanomizu University, 2-1-1 Otsuka, Bunkyo-ku, Tokyo 112-8610, Japan

Supporting Information

ABSTRACT: We report here a solid phase synthesis methodology that allows the incorporation of α-amino acids (**X**) into quinoline (**Q**) oligoamide foldamer sequences. Water-soluble hybrid oligoamides based on the $\mathbf{XQ_2}$ trimer repeat motif were shown to adopt helical conformations presenting α-amino acid side chains in a predictable linear array on one face of the helix. In contrast, sequences based on the **XQ** dimer motif expressed less well-defined behavior, most likely due to local conformational variability precluding long-range order. Also presented is a full structural investigation by NMR of a dodecameric $\mathbf{XQ_2}$-type foldamer containing four different amino acid residues (Lys, Ala, Asp, and Ser).

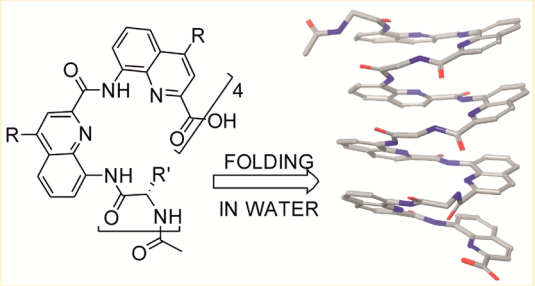

INTRODUCTION

The peptide backbone, consisting of the 20 α-amino acids provided by nature, is the primary structure that endows proteins with their ability to fold and results in their unique properties in vivo. In particular, the diverse side-chains of α-amino acid building blocks play a crucial role in controlling protein folding,[1] protein−protein interactions,[2] and protein−ligand interfaces.[3] They are thus critical in allowing proteins to perform their wide variety of functions, among others, enzyme catalysis,[4] cellular signaling,[5] and molecular transport.[6] However, in isolation, short α-peptides are typically structurally unstable,[7] meaning side-chain orientations are spatially disorganized. This to a great extent complicates their potential use in biological applications.

Various strategies have been explored to overcome the conformational instability of α-peptides with particular emphasis on developing sequences that can form helical structures. These include analogues incorporating β-, γ-, or δ-amino acids,[7a,c,8] sterically restricted residues,[9] chiral directing groups,[10] and urea bonds,[11] or the presence of a covalent linkage between residues remote in a sequence (i.e., "stapling").[12] These peptide analogues can be broadly classified as "biotic" foldamers.[13] In contrast, an alternative strategy to develop a stable and well-defined secondary structure is to utilize backbones and folding modes that differ significantly from those of the biopolymer. Examples of these can be termed "abiotic" foldamers.[13]

To act as appropriate biopolymer mimics, abiotic foldamers must be able to display biotic-like functionality with a spatial organization compatible with biological targets. One key factor in achieving this is the predictability with which side-chain functional groups are arranged on the foldamer backbone. In this way, they can be made to closely mimic their respective placement in a biotic motif, such as a peptide α-helix. Significant progress toward this has been made by the group of Hamilton, using terphenyl-,[14] biphenyldicarboxamide-,[15] terephthalamide-,[16] and benzoylurea-based[17] scaffolds, by Wilson and co-workers with their oligobenzamide template,[18] the Rebek and Konig groups with their respective pyridazine/piperazine[19] and 1,4-dipiperazine benzene-based scaffolds,[20] and the Burgess group with a piperidine-piperidinone scaffold.[21]

Aside from being potential biopolymer mimics, one advantage of abiotic foldamers is precisely that they can afford access to functional group arrangements that are inaccessible to natural motifs, yet may also interact with biomolecules in unforeseen and interesting ways. Helical aromatic oligoamide foldamers consisting of 8-amino-2-quinolinecarboxylic acid having a side chain in position 4 "$\mathbf{Q}^{\mathbf{Xxx}}$" (where Xxx refers to three-letter code of analogous α-amino acids bearing the same side chain, when available) do not display side-chains in the same manner as α-helices, yet they feature key properties that make them promising peptidomimetics: they are medium sized (0.5−5.0 kDa), resistant to proteolytic degradation,[22] conformationally stable in a wide range of solvents and in particular in water[23] even at high temperatures,[24] and most importantly, they adopt well-defined, predictable conformations.[25] They have been shown to possess cell-penetrating properties,[22,26] and side-chain functionality can be tuned to afford high affinity for G-quadruplex DNA[27] or to interact with protein surfaces.[28]

A logical extension from exclusively abiotic peptidomimetics is to incorporate the exact functional groups that mediate protein−protein recognition, i.e., α-amino acids. A single amino

Received: November 21, 2015
Published: December 24, 2015

DOI: 10.1021/acs.joc.5b02671
J. Org. Chem. 2016, 81, 1137−1150

acid may for example be added at the extremity of an α-helix mimetic.[18c] When multiple α-amino acids are incorporated in an abiotic sequence to form a hybrid scaffold, the completely different folding principles of biotic and abiotic units may offer access to secondary structures distinct from those of biopolymers or synthetic homo-oligomers.[29] In other cases, the folding of abiotic units may be so effective that it forces α-amino acids to adopt conformations distinct from those found in peptides. We recently reported an example of this kind using helically folded quinoline oligoamides. Hybrid sequences consisting of a repeating motif of a single L-leucine residue followed by a quinoline dimer with 4-isobutoxy, leucine-like, side chains ($\mathbf{LQ^{Leu}_2}$, Figure 1(a)) have been found to adopt a

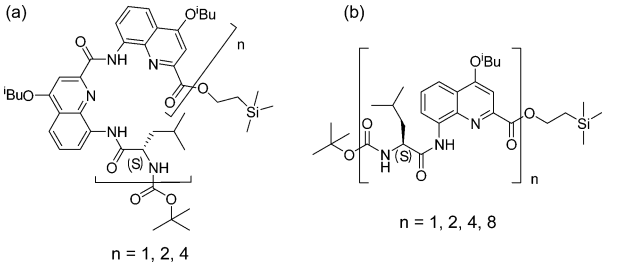

Figure 1. Structures of (a) $\mathbf{LQ^{Leu}_2}$ and (b) $\mathbf{LQ^{Leu}}$-type sequences.

stable right-handed helical conformation in organic solvents similar to that of quinolinecarboxamide homologous sequences despite the absence of features of aliphatic and aromatic building blocks, which would be expected to make their folding compatible a priori.[30] This ability of quinoline backbones to dictate folding was also observed with aliphatic blocks other than α-amino acids.[31] In contrast, sequences of a repeating L-leucine-quinoline dimer ($\mathbf{LQ^{Leu}}$, Figure 1(b)) were found to adopt a partially folded zigzag tape conformation with local conformational variability precluding long-range order. In other words, when there are too few quinoline residues to dominate the folding process, hybrid and potentially ill-defined behavior may result.[32] An interesting aspect of the $(\mathbf{LQ^{Leu}_2})_n$ helices is that the leucine residues are driven to form a linear array of side chain at ∼3.5 Å intervals, corresponding to the pitch of an aromatic helix. These arrays of side chains may be of use for the recognition of proteins or nucleic acid structures. In such an approach, a great advantage would lie in the commercial availability of α-amino acids: a wide variety of side chains may be incorporated without resorting to the potentially nontrivial and labor intensive synthesis of differently functionalized abiotic building blocks.

The purpose of the present investigation was twofold: develop a convenient synthetic methodology of $(\mathbf{XQ_2})_n$ oligomers with varied linear arrays of α-amino acids "X" and explore their conformation behavior in water. Because folding of aromatic oligoamide foldamers gives rise to extensive contacts between aromatic rings, it is greatly enhanced by hydrophobic effects.[23] We thus anticipated that the behavior of these hybrid sequences might vary in aqueous conditions. The previously reported solution phase synthesis of $(\mathbf{LQ^{Leu}_2})_n$ oligomers involved the preparation of water insoluble $\mathbf{LQ^{Leu}}$ and $\mathbf{LQ^{Leu}_2}$ intermediates. Synthesizing a variety of sequence analogues would thus be time-consuming, as it would require the production of a number of **XQ** and $\mathbf{XQ_2}$ intermediate building blocks. In contrast, a solid-phase methodology would be ideal in that it offers the advantage of allowing the stepwise incorporation of building blocks, including those that are commercially available.

Drawing on our experience with the solid-phase synthesis (SPS) of quinoline oligoamides,[31b] we describe here the development of a corresponding efficient methodology for the SPS of α-amino acid/quinoline hybrid sequences via the use of in situ formed α-amino acid chlorides. We have used this methodology to produce sequences based on **XQ** and $\mathbf{XQ_2}$ repeat motifs and investigated their conformations via CD and NMR studies. Polar side chains introduced on each Q unit were expected to diverge from the folded structures and, with the contribution of the main chain carboxylate terminus, to ensure water solubility of oligomers in the millimolar range despite the high aromatic content of the sequences. Our structural investigations include the full structural assignment by NMR of a dodecameric $(\mathbf{XQ_2})_4$ sequence, where four different α-amino acids have been incorporated, and the characterization of its helical conformation in aqueous medium (by convention, a monomer maybe a quinoline unit or an α-amino acid indifferently; an $(\mathbf{XQ_2})_4$ has 12 units and is thus considered to be a dodecamer).

RESULTS AND DISCUSSION

Methodology Development. The production of oligomers by SPS is particularly attractive in that it offers a method for rapidly generating sequence analogues where any monomer unit can be substituted for another without the laborious resynthesis of intermediates required by a more convergent solution phase approach. Although solid phase peptide synthesis methods are now widely standardized, the use of an SPS strategy for the production of foldamers based on 8-amino-2-quinolinecarboxylic acid is not without its challenges. The aromatic amine is a relatively poor nucleophile and thus coupling requires activation of monomers as acid chlorides and microwave assistance to be both rapid and essentially quantitative. We therefore anticipated the coupling of α-amino acids to this unit to be difficult. Indeed, in the solution-phase synthesis of $(\mathbf{LQ^{Leu}})_n$ and $(\mathbf{LQ^{Leu}_2})_n$ oligomers, leucine was required to be activated as the acid fluoride for it to be coupled to an 8-aminoquinoline monomer. Coupling to a quinoline dimer was found to be unfeasible, as it required heating, long reaction times, and resulted in significant racemization.[30]

Although our previous experience with SPS of quinoline oligoamides indicated that acid chlorides would be required for efficient coupling, the disadvantages of activating α-amino acids as their corresponding acid chlorides are widely reported.[33] We thus initially investigated some of the newer generations of coupling reagents, including aminiums (HATU),[34] phosphoniums (PyBroP),[35] propylphosphonic anhydride (T3P),[36] and the cyanuric chloride derivative DMTMM,[37] without success. This was also the case for both preformed acid fluorides (using cyanuric fluoride) and even those formed in situ (using DAST). We therefore returned to investigating the use of acid chlorides, reasoning that, if the activation and coupling process was short enough, it might be permitted without significant racemization. In this respect, the in situ generation of acid chlorides via the trichloroacetonitrile/triphenylphosphine methodology of Jang and co-workers[38] seemed to be an ideal choice; indeed, this procedure has also been subsequently applied to SPS.[39]

Initial trials appeared promising, and we thus carried out a brief study to assess coupling efficiency and compatibility of different side-chain functional groups between α-amino acids

DOI: 10.1021/acs.joc.5b02671
J. Org. Chem. 2016, 81, 1137−1150

and quinolines carrying different side chains (Figure 2). For this, we employed a resin-bound quinoline dimer (Scheme 1)

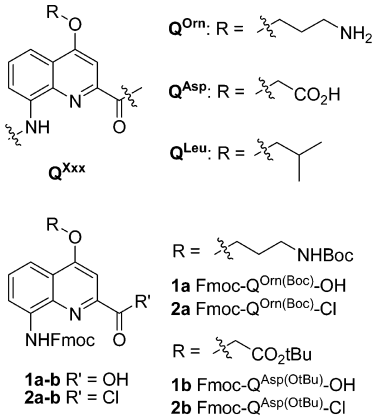

Figure 2. Structures of $\mathbf{Q}^{\mathbf{Xxx}}$ and Fmoc-protected quinoline monomers.

as starting material, synthesized using our SPS methodology from Wang-bromide resin.[31b] Fmoc-Lys(Boc)−OH was subsequently coupled using our initial unoptimized conditions: four equivalents of amino acid and four coupling cycles to afford, after resin cleavage, trimer **3c** in approximately 85% yield. Despite this initial success, we were concerned by two factors, the high excess of amino acid required and the possibility of racemization, especially in the case of cysteine.

We initially dealt with the first concern and were fortunate to discover that a key variable was the excess of triphenylphosphine, which if increased allowed complete coupling in the presence of only two equivalents of amino acid (in this case, the orthogonally protected Fmoc-Lys(Boc)−OH) after only two coupling cycles. This method proved effective with the majority of amino acids tested, although in some cases (e.g., serine), the number of coupling cycles needed to be increased. In all cases apart from α-amino-isobutyric acid (Fmoc-AiB−OH, which will be discussed later), coupling was complete after four cycles. Trimers **3a−g** were thus resynthesized using these conditions, affording crude yields from 50 to 70% and purities >90% by RP-HPLC. These products were also characterized by ^{1}H NMR and ESI-MS (see Experimental Section).

We assessed racemization by the addition of a second chiral center to allow detection of diastereoisomers. To each amino acid coupled to the quinoline amine via its acid chloride we coupled the same amino acid a second time (via HBTU/HOBt) with both the D and L forms of that amino acid. In each Fmoc-**LX**-**LX**-$(\mathbf{Q})_2$ tetramer produced, the byproduct resulting from racemization of the first amino acid residue (Fmoc-**LX**-**DX**-$(\mathbf{Q})_2$) would be an enantiomer of the Fmoc-**DX**-**LX**-$(\mathbf{Q})_2$ tetramer (with identical HPLC retention time and NMR signals) and vice versa. We considered it unlikely that racemization would occur during coupling of the second amino acid unit because this is not normally associated with aminium coupling reagents.[40] Detection of diastereomeric byproducts in crude Fmoc-$(\mathbf{X})_2$-$(\mathbf{Q})_2$ tetramers **4a−e** and **5a−e** was achieved by both RP-HPLC (Table 1) and ^{1}H NMR

Table 1. RP-HPLC Racemization Analysis of Fmoc-LX-LX-$(\mathbf{Q})_2$ and Fmoc-DX-LX-$(\mathbf{Q})_2$

tetramer	X	ratio product:byproduct[a]
4a	A	98:2
4b	K	N/A[b]
4c	D	99:1
4d	F	95:5
4e	S	98:2
5a	A	99:1
5b	K	N/A[b]
5c	D	94:6
5d	F	99:1
5e	S	98:2

[a]Determined by RP-HPLC. [b]Ratio could not be determined by RP-HPLC due to overlaying of the two peaks.

(see Supporting Information). As expected, chemical shifts and HPLC retention times of the Fmoc-**DX**-**LX**-$(\mathbf{Q})_2$ tetramers **5a−e** matched well with the putative byproducts of α-amino

Scheme 1. Solid Phase Synthesis of Various Fmoc-X$\mathbf{Q}_2$−OH Hybrid Tripeptides

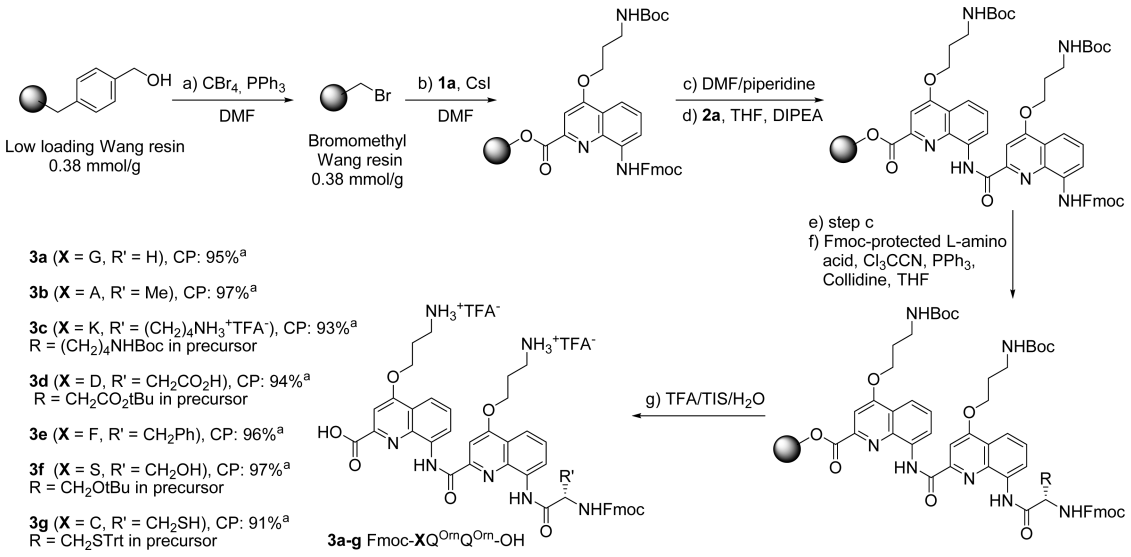

[a]CP stands for crude purity.

DOI: 10.1021/acs.joc.5b02671
J. Org. Chem. 2016, 81, 1137−1150

acid chloride racemization in Fmoc-**LX**-**LX**-$(\mathbf{Q})_2$, i.e., Fmoc-**LX**-**DX**-$(\mathbf{Q})_2$. The estimation of racemization was found to be robust and accurate. For example, tetramer **4a** showed approximately 2% byproduct formation by RP-HPLC, the peak of which corresponded well in terms of retention time with tetramer **5a** (Figure 3). Similarly, tetramer **5a** contained

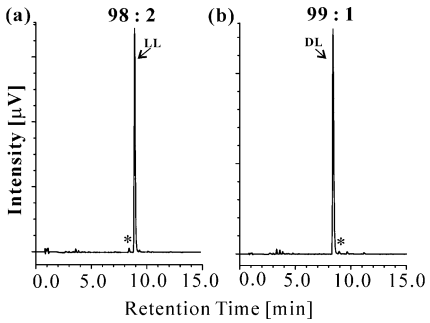

Figure 3. RP-HPLC chromatogram of crude products (a) **4a** and (b) **5a**. LL = Fmoc-Ala-Ala-$(Q)_2$−OH, DL = Fmoc-DAla-Ala-$(Q)_2$−OH, and * = putative byproduct of racemization during in situ acid chloride coupling.

approximately 1% byproduct formation, the peak of which corresponded well with **4a**. The incidence of racemization for each amino acid incorporated was similar for the D and L isomers with small differences (<5%) probably resulting from the small scale at which these trials were carried out. For cases in which retention times were too similar to distinguish each diastereomer by C_{18}-RP-HPLC (e.g., **4b** and **5b**), ^{1}H NMR showed them to possess distinct differences in chemical shifts in their aromatic and amide regions (Figure 4). In some cases, no

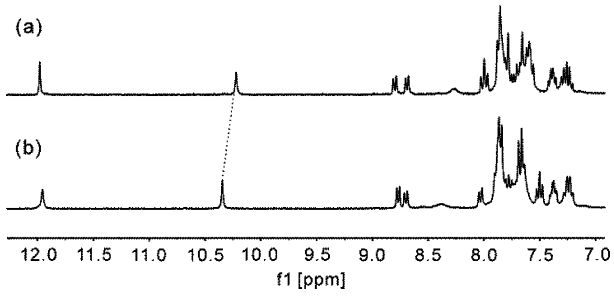

Figure 4. Amide and aromatic region of ^{1}H NMR spectra (300 MHz) of crude (a) **4b** and (b) **5b** in DMSO-d_6 showing a single set of signals in each instance.

signals associated with the other diastereoisomer were visible, indicating racemization was negligible. Overall, racemization was kept under acceptable levels considering its known occurrence when using acid chloride activation. One exception was cysteine for which racemization was found to be too high to be of practical use (not shown).

We were keen to develop a methodology to incorporate the α,α-disubstituted AiB residue into hybrid foldamer sequences, as it is well-known for inducing helical folding in α-peptides and might lead to distinct behavior when mixed with an abiotic backbone. Probably due to steric hindrance, in situ acid chloride formation for the introduction of Fmoc-AiB led to incomplete coupling. We thus decided to adopt a fragment condensation methodology for incorporation of this residue. An AiB dimeric block was synthesized from the previously reported methyl 8-amino-4-isobutoxyquinoline-2-carboxylate **6** (Scheme 2). In this case, the isobutoxy side-chain was chosen for its well-

Scheme 2. Synthesis of Fmoc-AiB-Q^{Leu}−OH Dimer Building Block 8

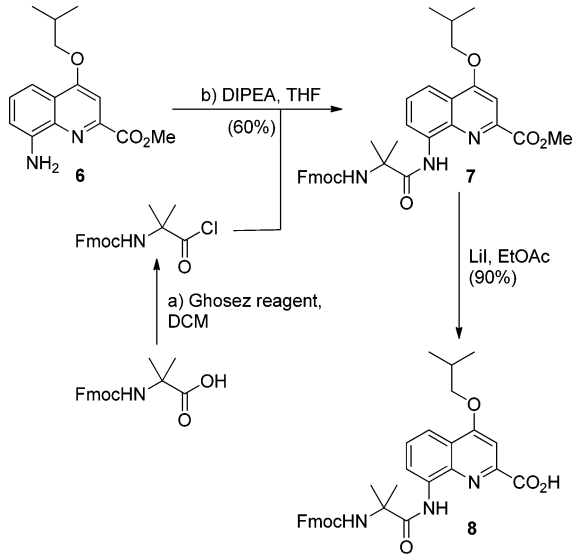

documented ability to provide solubility in organic solvents,[41] thus reducing the risk of poor solubility of synthetic intermediates. Fmoc-AiB−OH was converted to its corresponding acid chloride via the use of the Ghosez reagent (1-chloro-*N*,*N*,2-trimethyl-1-propenylamine) and subsequently coupled to amine **6** to afford dimer **7** in 60% yield. The relatively modest yield in this case serves to illustrate the difficulty in coupling even reactive species, such as acid chlorides, to the relatively unreactive quinoline 8-amino group, and thus highlights the utility of microwave assistance during SPS. Conversion of the methyl ester to corresponding acid **8** was carried out in high yield by treatment with LiI, a method which avoids removal or modification of the terminal N^{α}-Fmoc group.

Preliminary tests with this dimer building block indicated that the HBTU/HOBt system could potentially be used in conjunction with microwave assistance. However, we were concerned that, for longer sequences, coupling efficiency might be reduced, and thus for SPS of the 13mer **9**, we employed our usual conditions[31b] for activation of **8** as the acid chloride followed by microwave-assisted coupling (Scheme 3). This afforded the final product in 39% yield after column chromatography. The fragment condensation approach thus proves useful for those monomers that cannot be coupled in high yield during SPS. However, it was not readily helpful for the particular case of cysteine as even the solution phase coupling to a quinoline monomer led to extensive racemization.

To summarize, our SPS method for coupling α-amino acids to the quinoline aromatic amine was found to be highly efficient and led in most instances to negligible racemization. To access more difficult hybrid sequences (e.g., containing α-amino acids with higher steric hindrance at the α-carbon), the strategy of using preformed XQ dimer blocks appears to be a viable alternative. Both methods were found to be fully compatible with our microwave-enhanced SPS methodology.

SPS of $(XQ)_n$ and $(XQ_2)_n$ oligoamide sequences via the in situ acid chloride methodology. To confirm the utility

DOI: 10.1021/acs.joc.5b02671
J. Org. Chem. 2016, 81, 1137−1150

Scheme 3. SPS of 13mer 9 from Dimeric Unit 8

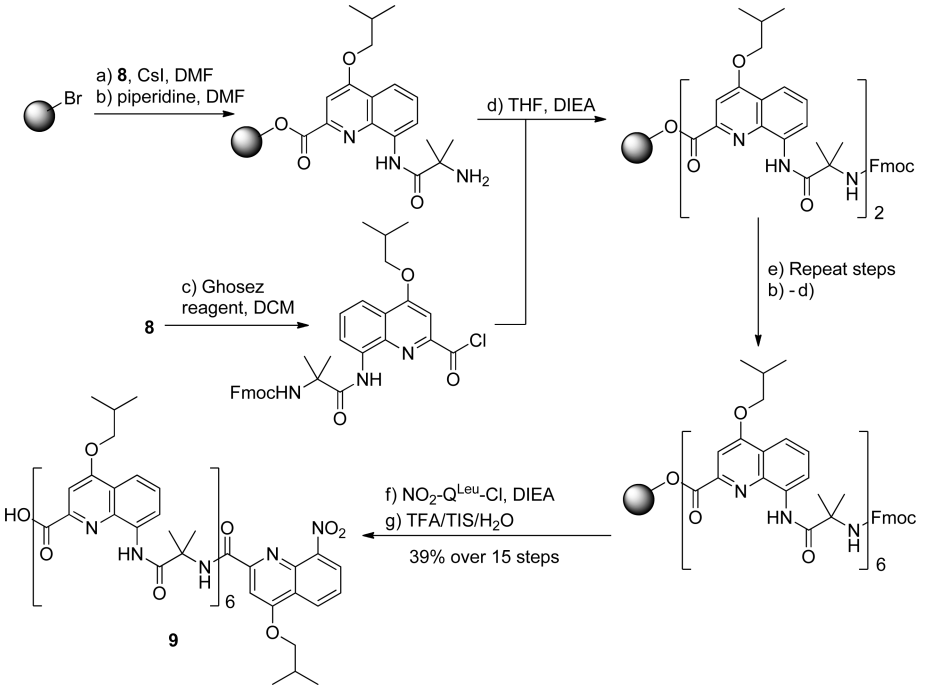

Scheme 4. Solid Phase Synthesis of Water-Soluble XQ- and XQ_2-Type Hybrid Sequences

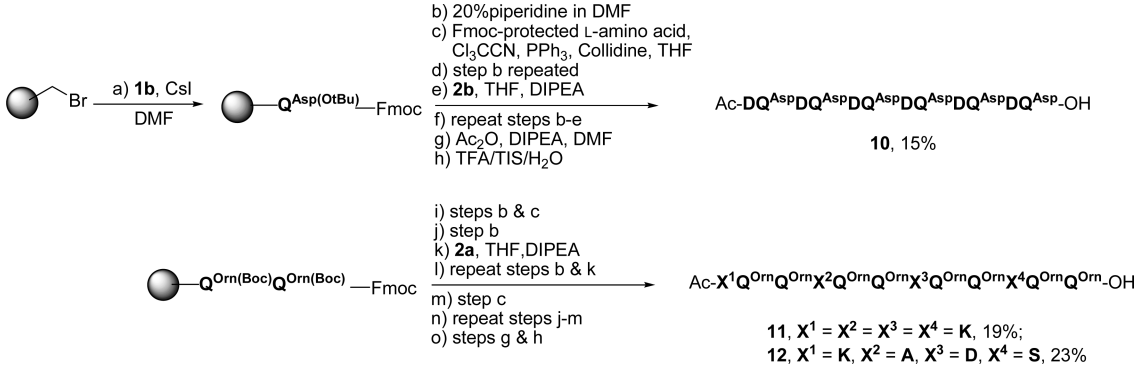

of our in situ acid chloride coupling method, we first aimed to synthesize sequences based on a dimeric (**XQ**) repeat motif. Foldamers based on this motif had previously been shown in organic solvents to adopt a partially folded zigzag tape conformation with local conformational variability precluding long-range order.[32d] Considering that hydrophobic effects play a large part in stabilizing the conformations of aromatic oligoamide foldamers in aqueous conditions, we were curious to see if the conformations of fully water-soluble $(\mathbf{XQ})_n$ sequences were any different from their organic-soluble counterparts.

The first sequence **10** was therefore an $(\mathbf{XQ})_n$-type 12mer combining Asp residues with quinolines bearing "Asp-like" side-chains to provide aqueous solubility at neutral or near-neutral pH while minimizing the risk of aggregation associated with mixing side-chains of different charge types (e.g., Asp and Lys). In brief, low-loading (0.38 mmol g^{-1}) Wang resin was converted to its corresponding bromide using the reported procedure[31b] and loaded with the first Fmoc-Q^{Asp} monomer unit (Scheme 4). Fmoc deprotection was carried out using 20% v/v piperidine in DMF at 25 °C and Fmoc-Asp(tBu)−OH incorporated via its in situ-formed acid chloride using our optimized methodology. Coupling of the Fmoc-Q^{Asp} monomer unit to the aliphatic amine was carried out through the preformed acid chloride as previously described, and synthesis continued to afford the final sequence. Capping of the N-terminal amine was carried out using acetic anhydride and the crude product (23.5 mg, 51% crude yield; purity by RP-HPLC: 60%) cleaved from the resin using a solution of TFA/TIS/H_2O (95:2.5:2.5 v/v/v). Purification by RP-HPLC afforded the final pure product in a yield of 15% over 27 steps.

We also wanted to extend our methodology to sequences based on the $\mathbf{XQ_2}$ trimer repeat motif, as an organic soluble analogue was reported to form well-defined helices.[30] However, we anticipated that their sequence might be slightly more of a challenge than with **XQ** repeat motifs due to the incorporation of the additional coupling between quinoline units. To vary side-chain functionality from sequence **10**, we chose a sequence that combined Lys with quinolines bearing "Orn-like" side-chains.[31b]

Fmoc-$(Q^{Orn})_2$-Wang was synthesized using the methodology as previously described with the Fmoc group deprotected and Fmoc-Lys(Boc)−OH incorporated using our optimized in situ acid chloride method (Scheme 4). The sequence was then

DOI: 10.1021/acs.joc.5b02671
J. Org. Chem. 2016, 81, 1137−1150

continued in the same fashion to produce the 12mer with the terminal Fmoc removed, the resulting amine acetylated, and the product cleaved from the resin in the same manner as for the $(XQ)_n$ sequence. The resulting crude product was purified by RP-HPLC to afford sequence **11** in a yield of 19% over 27 steps. To further test the reproducibility of our methodology and also to provide a sequence more amenable to full NMR assignment, we also synthesized compound **12**, which incorporated Lys, Ala, Asp, and Ser residues. This sequence was afforded after RP-HPLC purification with a yield of 23% over 27 steps.

Structural Analysis of $(XQ)_n$ and $(XQ_2)_n$ Oligoamide Sequences. For $(XQ)_n$ sequences, we were first interested to see if their backbone flexibility and lower content of aromatic units could be overcome by solvophobic effects in protic solvents, inducing folding into more ordered conformations than observed in organic solvents. For $(XQ_2)_n$ sequences, we were intrigued to see if protic solvents induced any changes in conformation over that which had been previously seen in the reported crystal structure of $(LQ^{Leu}{}_2)_4$ from organic solvents. We first turned to CD analysis as a rapid way to detect potential folding behavior. The 12mers **10** and **11** were analyzed as examples of $(XQ)_n$ and $(XQ_2)_n$ sequences, respectively. Figure 5 shows that for **11**, the characteristic bands at approximately

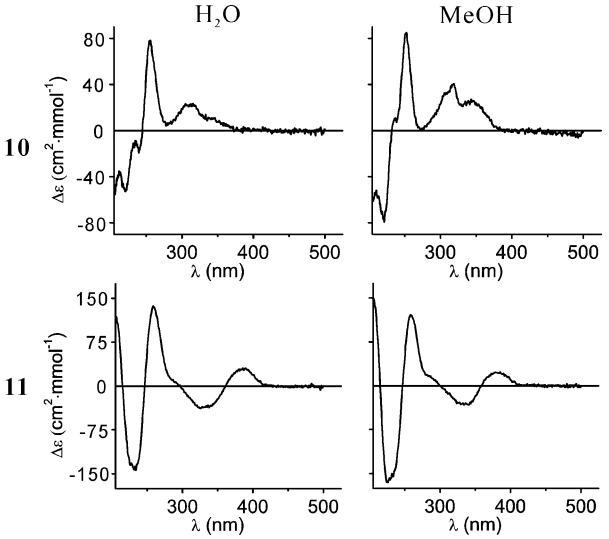

Figure 5. CD spectra of **10** and **11** in H_2O and MeOH at 20 °C (concentration: 30 μM).

380 nm associated with quinoline stacking (and therefore probable helical conformation) are present in both methanol and water. In addition, this CD spectrum also matches well with that reported for $(LQ^{Leu}{}_2)_4$, where the positive signal of the band at 380 nm indicates the same right-handed (*P*) helix sense.[30] A similar CD was also recorded for compound **12** (see Supporting Information), indicating the low impact of side-chain functionality on this conformational preference. In contrast, we were disappointed to see that the CD spectrum for **10** lacks bands at 380 nm, and its similarity with the CD spectrum of $(LQ^{Leu})_4$ indicates that this sequence does not appear to fold into a helical conformation even in protic solvents.

We then turned to the ^{1}H NMR spectra of **10** and **11** to provide more detailed information about their folding. The aromatic region displayed in Figure 6 shows a single set of

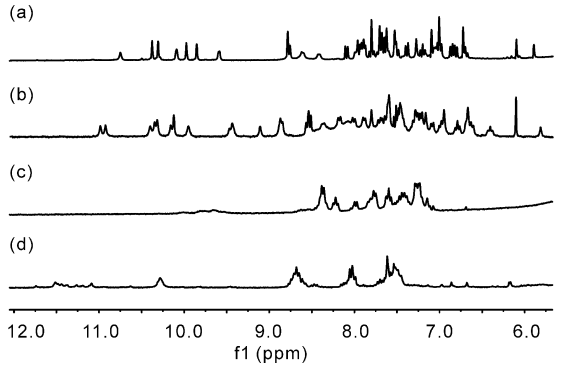

Figure 6. Part of the ^{1}H NMR spectra (300 MHz) of **10** and **11** showing aromatic amide (9–12 ppm), aliphatic amide, and aromatic proton resonances (6–10 ppm) in protic solvents at 25 °C for (a) **11** in H_2O/D_2O (9:1 v/v), (b) **11** in CD_3OH, (c) **10** in H_2O/D_2O (9:1 v/v), and (d) **10** in CD_3OH.

sharp signals for compound **11** in both H_2O/D_2O (9:1) and d_3-MeOH (Figure 6a and 6b, respectively) with resonances spread over a wide chemical shift range and with minimal exchange of amide protons. This indicates that the sequence is in a single well-defined conformation; upfield shifting of some signals also indicates the effect of aromatic $\pi-\pi$ stacking associated with helical folding as normally seen in quinoline-based aromatic oligoamide foldamers. Interestingly, the signals of **11** are significantly sharper at 25 °C than those of the analogous $(LQ^{Leu}{}_2)_4$ sequence in solvents such as $CDCl_3$, the spectra of which could only be sharpened by cooling to low temperatures.[30] This difference probably reflects the increased conformational stability of this foldamer type in protic solvents due to the high contribution of hydrophobic forces toward folding and therefore the high impact of solvent on stability of the resulting helix. Furthermore, temperature experiments with **11** showed that heating in CD_3OH resulted in signal broadening, whereas in H_2O/D_2O (9:1), this was not observed (see Supporting Information). This high stability in aqueous conditions also matches well with our previous experience regarding the solvent dependence of handedness inversion kinetics in quinoline oligoamide foldamers.[42]

In contrast, the spectra of **10** show broad signals at 25 °C in both H_2O/D_2O (9:1) and CD_3OH (Figure 6c and 6d, respectively) with evident solvent exchange of many amide protons. In addition, the former solvent appears to afford a single set of signals, whereas in the latter, a minor species is apparent. Temperature experiments (see Supporting Information) revealed that, in both solvents, lower temperatures resulted in signals becoming broader and the appearance of additional signals. Increasing the temperature resulted in convergence of signals. This appearance of additional sets of signals can most likely be attributed to nonspecific aggregation and perhaps indicates the higher availability of hydrophobic surfaces because they are less involved in folding of the sequence. To summarize, the spectra of **10** indicate the presence of multiple poorly folded and thus solvent accessible conformations with the higher availability of aromatic surfaces permitting nonspecific aggregation.

Assignment and Conformational Analysis of Compound 12 by NMR. To delve further into the solution-state folding behavior of the $(XQ_2)_n$-type foldamers, we carried out a detailed analysis of compound **12**, a 12mer in which four different amino acid residues had been incorporated. COSY

DOI: 10.1021/acs.joc.5b02671
J. Org. Chem. 2016, 81, 1137–1150

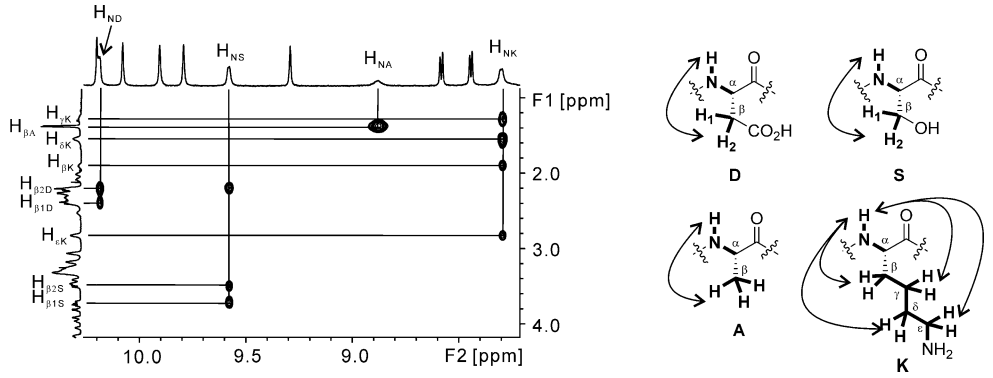

Figure 7. Excerpt from $^{1}H—^{1}H$ TOCSY spectrum of **12** in H_2O/D_2O (9:1 v/v) at 25 °C (700 MHz) indicating the correlations between aliphatic amide proton (H_{NX}) and side-chain methylene protons (H_X) of each amino acid. Double-headed arrows indicate the observed correlations.

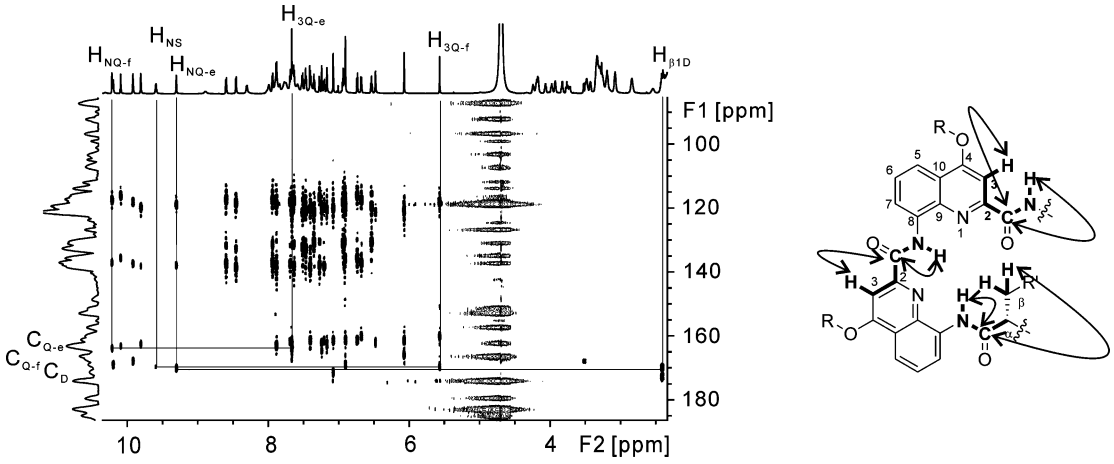

Figure 8. Excerpt from $^{1}H—^{13}C$ HMBC spectrum of **12** in H_2O/D_2O (9:1 v/v) at 25 °C (700 MHz) indicating the correlations involved in assigning the -DQQS- fragment of the sequence. Double-headed arrows indicate the observed correlations.

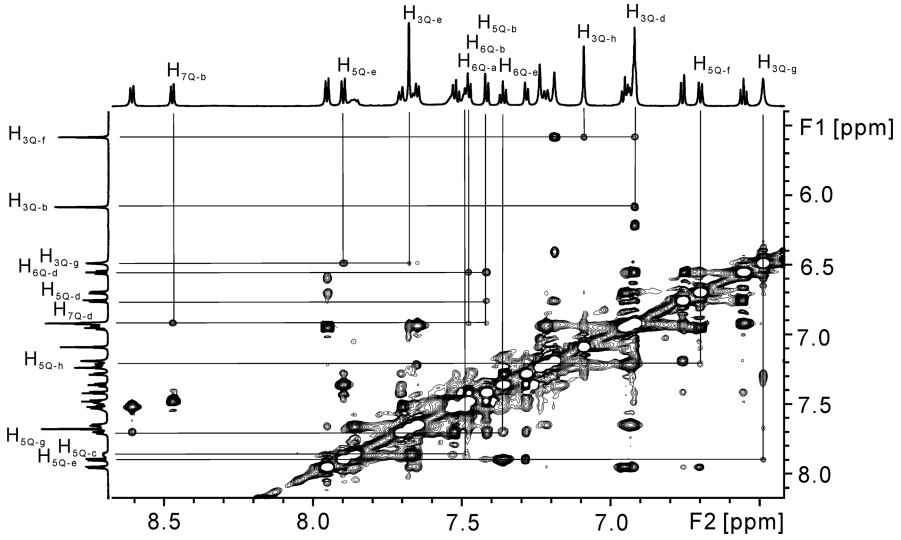

Figure 9. Excerpt from $^{1}H—^{1}H$ NOESY spectrum of **12** in D_2O at 25 °C (800 MHz) showing the NOE correlations between aromatic protons of quinolines at *i* and *i* + 3.

and TOCSY experiments (in H_2O/D_2O (9:1)) permitted assignment of amino acid and quinoline protons as demonstrated in Figure 7 (for numbering rules, see Supporting Information).

Quinoline protons could also be separated into eight discrete groups, corresponding to each quinoline unit. HMBC data was then used to establish correlations between each quinoline amide NH with C7 of the ring, which could further provide H5.[25b] In the same manner, H3 could be correlated to C4 and then back to H5. Finally C5 could be correlated to H7 (see Supporting Information). Once this was completed for each quinoline, it was then correlated with the surrounding amino

DOI: 10.1021/acs.joc.5b02671
J. Org. Chem. 2016, 81, 1137−1150

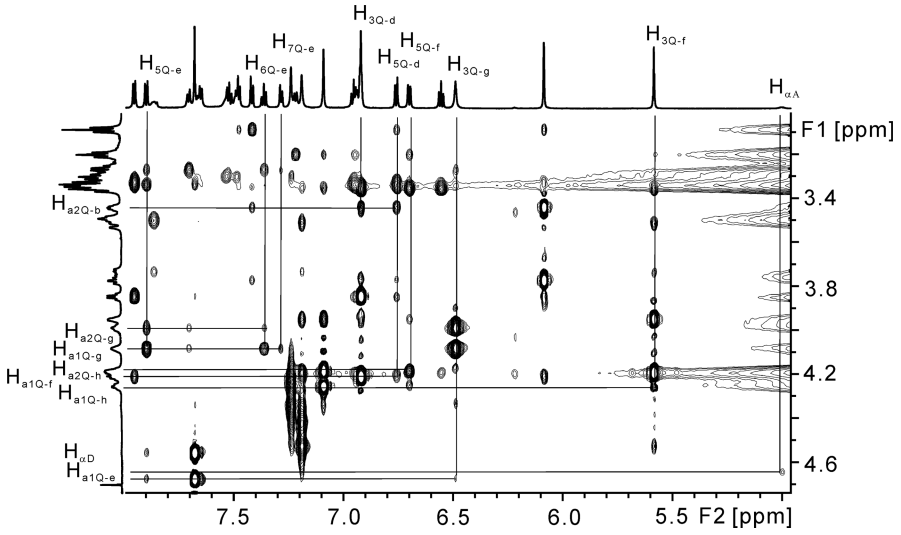

Figure 10. Excerpt from ^{1}H—^{1}H NOESY spectrum of **12** in D_2O at 25 °C (800 MHz) showing the NOE correlations between quinoline side-chain methylene protons and aromatic protons of quinolines at i + 3.

acid residues to provide sequence information. Figure 8 provides the example of the -DQQS- fragment: the Asp carbonyl carbon (C_D) was correlated to the adjacent quinoline (quinoline 'e') amide NH ($H_{NQ\text{-}e}$), which then provided the quinoline H3 position ($H_{3Q\text{-}e}$), which had been assigned. This could then be correlated to the quinoline carbonyl carbon ($C_{Q\text{-}e}$) and then on to the amide NH of the next quinoline unit ($H_{NQ\text{-}f}$). Correlations continued in the same manner to provide the serine amide NH (H_{NS}). Further details of all correlations are outlined in the Supporting Information.

Once the sequence was fully assigned, NOESY experiments were used to provide information on the sequence conformation. Important correlations were made between i and i + 3 quinoline units, and position H3 was particularly useful as a clearly distinguished singlet. For example, correlations can be seen between $H_{3Q\text{-}f}$ with both $H_{3Q\text{-}d}$ and $H_{3Q\text{-}h}$, indicating their closeness in space, and thus suggesting they are stacked in sequence (Figure 9). In a similar manner, methylenes of the quinoline 4-position side-chain proximal to the ether (3.4−4.2 ppm) were also useful in that they were found to have strong correlations with i + 3 quinoline ring protons (Figure 10).

Encouraged by the substantial number of NOE correlations that appeared to support a helical conformation, we made the further step to generate a molecular model based on these data. After eliminating overlapping or ambiguous signals, NOE correlations were first integrated and further converted to distance information according to the reported formula.[43] Then, an ill-folded structure of **12** with a right-handed helical twist was energy minimized using MacroModel using distance information as constraints. This yielded a first helical structure that was then randomly modified and again minimized by the same method to generate a second molecular model. This process was repeated 19 times to obtain 20 molecular models for superposition and RMSD calculation (Figure 11e). Associated RMSD data show that the sequence backbone demonstrates considerable stability. Panels a−c in Figure 11 show one of the 20 models of compound **12**: in agreement with CD data, it adopts a right-handed helical arrangement with close resemblance to the crystal structure of $(\mathbf{LQ_2})_4$ previously reported.[30] Repeated attempts were made to apply the NOE data to a left-handed structure with no success. Each $\mathbf{XQ_2}$ unit spans approximately one turn (pitch of 4.1 Å) resulting in an arrangement of the α-amino acid side-chains on one face of the helix. However, rather than being directly overlaid, they are offset from each other by a number of degrees, resulting in a diagonal array of side-chains down the helix axis. The Cα-Cα distances between consecutive α-amino acids starting from the N-terminus are 5.0, 4.4, and 5.0 Å, respectively, which are slightly smaller than the average distance (6.3 Å) in an α-helix. One significant difference from the crystal structure of $(\mathbf{LQ^{Leu}_2})_4$ is that, in this case, the α-amino acid amide NH groups do not point directly toward the helix axis. Indeed, the NH of alanine appears to form a hydrogen bond with the carbonyl CO of lysine, setting alanine with ϕ = −145.7° and ψ = 40.3°. It is quite normal for peptides with a secondary structure of β-sheet or right-handed α-helix to have such high negative ϕ values. However, the coordinate falls (combining the small positive ψ value) in the allowed area of β-sheet according to Ramachandran plot. This tilting of the α-amino acid amide function to planes parallel to the helix axis was previously suggested by an energy-minimized molecular model of $(\mathbf{LQ^{Leu}_2})_4$ that was slightly different from its crystal structure.[30] However, this model suggested that the amide NHs would tilt down in the direction of the C-terminus, forming hydrogen bonds with the quinoline i + 2 amide carbonyl. In the model of **12**, it can be seen that the α-amino acid amide NHs are instead tilted upward toward the N-terminus (apart from the NH of lysine, which due to being at the N-terminus appears to be involved in a hydrogen bond with the CO of alanine). In the case of serine, this effect is severe enough that it results in a slight distortion of the backbone π−π stacking, increases the serine ϕ angle to −78.4°, and results in the NH proton being in close proximity (3.0 Å) to H3 of the neighboring quinoline unit 'f' ($H_{3Q\text{-}f}$). This distance was confirmed by analysis of the appropriate correlations via further ROESY experiments (Figure 11d). This distortion is assumedly compensated by the formation of three hydrogen bonds: between the carbonyl of quinoline 'f' with i + 2 and i + 3 quinoline amide NHs and the C-terminal carboxylic acid.

Variable temperature NMR experiments with the organic-soluble analogue $(\mathbf{LQ^{Leu}_2})_4$ previously demonstrated the

DOI: 10.1021/acs.joc.5b02671
J. Org. Chem. 2016, 81, 1137−1150

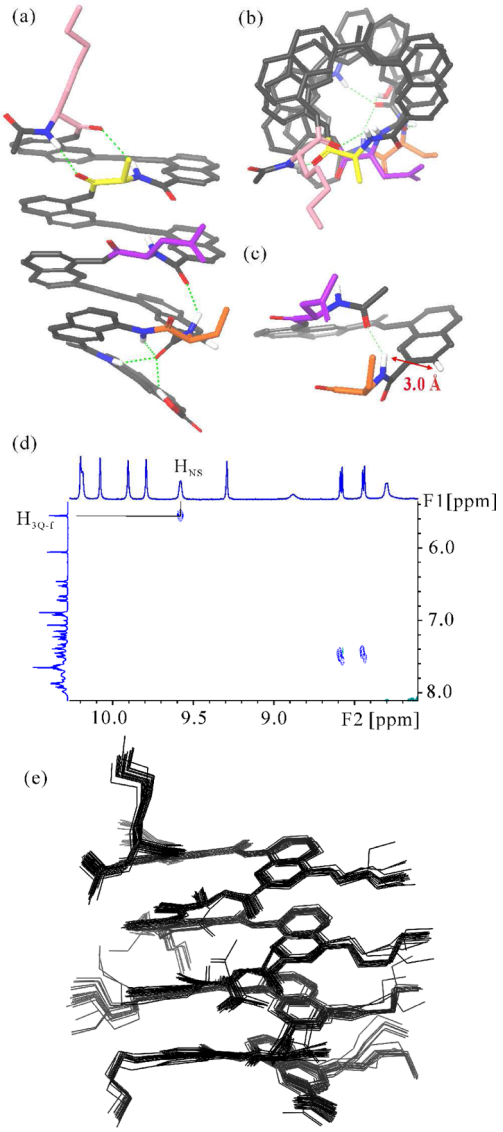

Figure 11. An NOE data-based molecular model: (a) side view; (b) top view; (c) segment showing distance between H_{NS} and $H_{3Q\text{-}f}$ of **12**; (d) part of ROESY spectrum of **12** in H_2O/D_2O (9:1 v/v) at 25 °C (700 MHz) showing the corresponding correlation between the amide NH of Ser (H_{NS}) and H3 of the neighboring quinoline 'f' ($H_{3Q\text{-}f}$) observed in the molecular model; and (e) superposition of 20 energy-minimized structures. Key N, O, and H atoms are shown in blue, red, and white, respectively. Lys, Ala, Asp, and Ser residues are shown in pink, yellow, purple, and orange, respectively. Quinolines are shown in gray with side-chains removed for clarity. Putative hydrogen bonds are shown as dashed green lines. Double-headed arrow in red (c) indicates the distance between H_{NS} and $H_{3Q\text{-}f}$. All hydrogen atoms of the 20 superposed structures have been removed for clarity.

existence of two nonaggregated, concentration-independent and solvent-dependent helical states of similar handedness equilibrating slowly on an NMR time scale, which were assigned to the state observed in the crystal and another suggested by molecular modeling.[30] Our study of water-soluble **12** shows that only one species prevails in water and provides direct evidence for a helical conformation slightly differing from that observed in the solid state. In particular, in water, a number of different hydrogen bond arrangements are possible other than the $i/i-1$ hydrogen bonding network seen in the crystal structure of $(\mathbf{LQ_2})_4$.

CONCLUSIONS

An efficient microwave-assisted solid phase methodology has been developed allowing the incorporation of a range of α-amino acids into quinoline oligoamide sequences with negligible racemization (<2%) in most cases. For difficult cases such as AiB, an alternative segment condensation strategy was also validated. Both methods are fully compatible with our existing strategy for SPS of quinoline oligoamides. CD and NMR analysis demonstrated that, even in protic solvents, sequences based on an **XQ** dimer repeat unit do not fold into a single defined conformation with the associated solvent-accessibility of the hydrophobic aromatic surfaces appearing to drive nonspecific aggregation at lower temperatures. In contrast, sequences based on an $\mathbf{XQ_2}$ trimer repeat unit demonstrate folding into a single well-defined conformation in protic solvents at a range of temperatures with no evidence of aggregation behavior. A dodecameric $\mathbf{XQ_2}$-type foldamer containing four different amino acid residues (Lys, Ala, Asp, and Ser) was fully assigned by NMR in aqueous medium, and calculated distances were used to generate a molecular model. This demonstrated that the sequence adopts a right-handed helical arrangement with the four amino acid residues projecting side chains in an array on one face of the helix. Putative hydrogen bonds were shown to be different from those seen in the crystal structure of the organic-soluble analogue $(\mathbf{LQ^{Leu}_2})_4$ and shed further light on conformational preferences of these hybrid sequences under different conditions. Further work will focus on diversifying side-chain functionality of the $(\mathbf{XQ_2})_n$-type hybrid foldamers and studying their application toward targeting biological systems.

EXPERIMENTAL SECTION

General Procedures. All of the reagents and solvents were obtained from commercial sources, including Fmoc-protected amino acids, low loading Wang resin, and Ghosez reagent (1-chloro-*N*,*N*,2-trimethyl-1-propenylamine). *N*,*N*-Diisopropylethylamine (DIEA) was distilled over calcium hydride. Analytical grade organic solvents were used for solid phase synthesis. Anhydrous THF and CH_2Cl_2 for solution and solid phase synthesis were dispensed from a solvent purification system. HPLC grade acetonitrile and Milli-Q water were used for RP-HPLC analyses and purification. SPS was carried out manually at atmospheric pressure using a CEM Discover microwave oven and SPS station and in the proprietary reactor vessels. The temperature of microwave-assisted reactions was controlled by an optical fiber probe internal to the reaction mixture linked to an IR detector. ^{1}H NMR spectra were recorded at 300, 400, 700, or 800 MHz; 2D NMR spectra were recorded at 400, 700, or 800 MHz, and $^{13}C\{^1H\}$NMR spectra were recorded at 300 MHz. Chemical shifts are reported in ppm relative to the residual solvent signal of DMSO-d_6 (δ 2.50), CD_3OH (δ 3.31), $CDCl_3$ (δ 7.26, 77.2), or to the reference signal of TMS (δ 0.00) from 10 μM 3-(trimethylsilyl)-1-propanesulfonic acid sodium salt in CD_3OH, D_2O, or H_2O/D_2O (9:1). Abbreviations used for signal multiplicities are s, singlet; d, doublet; t, triplet; q, quartet; m, multiplet or overlapped signals; and br, broad. All coupling constants are reported in hertz (Hz). Silica gel chromatography was performed with Si 60 and thin layer chromatography with Si 60 F254 plates. RP-HPLC analyses were carried out on a C_{18} gravity column (4.6 × 100 mm, 3 μm) at 1.5 mL/min with running solvents: Milli-Q water containing 0.1% v/v TFA (solvent A), CH_3CN containing 0.1% v/v TFA (solvent B), 12.5 mM NH_4Ac-NH_4OH in Milli-Q water, adjusted to pH 8.5 (solvent C), and CH_3CN (solvent D). Gradients for analytical RP-HPLC were as follows: 20−50% B over 15 min (System A); 20−40% B over 10 min (System B); 30−50% B over 10 min (System C); 13−18% B over 10 min (System D); and 8−13% D over 10 min (System E). Systems A−D used solvent A as aqueous component, and System E used solvent C as aqueous

DOI: 10.1021/acs.joc.5b02671
J. Org. Chem. 2016, 81, 1137−1150

component. Column effluent was monitored by UV detection at 214, 254, and 300 nm with a diode array detector. Purification of oligoamides was performed at 4 mL/min on a C_{18} column (21 mm × 125 mm, 5 μm) by semipreparative RP-HPLC. The running solvents of semipreparative RP-HPLC were the same as analytical RP-HPLC. Gradients for semipreparative RP-HPLC were as follows: 15−20% B over 20 min (System F) and 10−15% D over 20 min (System G). System F used solvent A as the aqueous component, and System G used solvent C as the aqueous component. Monitoring was performed by UV detection at 254 and 300 nm with a diode array detector. High resolution electrospray ionization time-of-flight (ESI-TOF) mass spectra were measured in the positive ion mode on a TOF spectrometer.

Synthetic Methods. Fmoc-$Q^{Orn(Boc)}$−OH, Fmoc-$Q^{Asp(OtBu)}$−OH, H_2N-Q^{Leu}-OMe, and O_2N-Q^{Leu}−OH were synthesized as previously reported.[22,26,31b,44] Procedures for resin loading, Fmoc removal, quinoline acid chloride activation and couplings, and resin cleavage were also carried out as previously reported.[31b]

General Method for Coupling with HOBt/HBTU. The corresponding H_2N-oligomer-Wang resin (exemplified by 0.0038 mmol scale, 1 equiv) was washed with anhydrous DMF and then suspended in 0.3 mL of anhydrous DMF, to which was added a solution of Fmoc-protected amino acid or dimer block (0.0114 mmoL, 3 equiv), HBTU (0.0114 mmoL, 3 equiv), HOBt (0.0114 mmoL, 3 equiv), and anhydrous DIEA (0.0114 mmoL, 3 equiv) in anhydrous DMF (0.3 mL). The mixture was then treated with microwaves (25 W, 70 °C, 10 min). The resin was washed briefly with anhydrous DMF, and the process was repeated once.

General Method for N-Terminal Acetylation. The corresponding H_2N-oligomer-Wang resin (exemplified by 0.0038 mmol scale, 1 equiv) was washed briefly with anhydrous DMF and then suspended in 0.3 mL of anhydrous DMF, to which was added anhydrous DIEA (0.076 mmol, 20 equiv) and acetic anhydride (0.038 mmol, 10 equiv) in that order. The mixture was then stirred at 25 °C for 20 min. The resin was washed briefly with anhydrous DMF, and the process was repeated once.

General Method for in Situ Acid Chloride Coupling of α-Amino Acids using TCAN/PPh_3 As Exemplified by Synthesis of Compound ***3a****.* H_2N-$Q^{OrnBoc}Q^{OrnBoc}$-Wang resin was synthesized on a 0.0076 mmol scale (20 mg of Wang resin, loading 0.38 mmol/g) via the previously reported SPS methodology.[31b] NH_2-$Q^{OrnBoc}Q^{OrnBoc}$-Wang resin was washed briefly with anhydrous THF and then suspended in 0.5 mL anhydrous THF. 2,4,6-Collidine (8.7 μL, 0.066 mmol, 8.7 equiv), Fmoc-Gly-OH (4.5 mg, 0.015 mmol, 2.0 equiv), PPh_3 (21.9 mg, 0.084 mmol, 11 equiv), and TCAN (6.6 μL, 0.066 mmol, 8.7 equiv) were dissolved in 0.5 mL of anhydrous THF in that order and added to the resin immediately, which was then treated with microwaves (50 W, 50 °C, 15 min). The resin was then washed thoroughly with DMF, DCM, and DCM/MeOH (1:1), dried, and desiccated. Cleavage of the resin (TFA/TIS/H_2O, 95:2.5:2.5, 2 h, 25 °C) afforded 5.6 mg (75%) crude product (95% purity as determined by RP-HPLC). RP-HPLC (System A) R_t = 9.37 min. ^{1}H NMR (300 MHz, DMSO-d_6): δ 12.01 (s, 1 H), 10.39 (s, 1 H), 8.72−8.80 (m, 2 H), 8.00 (d, J = 7.8 Hz, 1 H), 7.60−7.90 (m, 14 H, -NH_3^+ included), 7.26−7.45 (m, 4 H), 7.08−7.25 (m, 2 H), 4.50−4.60 (m, 2 H), 4.40−4.50 (m, 2 H), 3.50−4.10 (m, 5 H), 3.00−3.20 (m, 4 H), 2.10−2.30 (m, 4 H). HRMS: calcd for $C_{43}H_{42}N_7O_8$ [M + H]$^+$ 784.3095; found 784.3127.

Compound 3b. The same procedure as described for the synthesis of **3a** was applied with the exception that the coupling with TCAN/PPh_3 was repeated once to obtain 5.0 mg (66%) of crude product (97% purity as determined by RP-HPLC). RP-HPLC (System A) R_t = 9.30 min. ^{1}H NMR (300 MHz, DMSO-d_6): δ 11.96 (s, 1 H), 10.50 (s, 1 H), 8.78 (d, J = 7.8 Hz, 1 H), 8.64 (d, J = 7.5 Hz, 1 H), 7.99 (d, J = 8.4 Hz, 1 H), 7.70−7.85 (m, 12 H, -NH_3^+ included), 7.65 (s, 1 H), 7.60 (t, J = 8.1 Hz, 1 H), 7.25−7.35 (m, 4 H), 7.05−7.20 (m, 2 H), 4.50−4.60 (m, 3 H), 4.38−4.47 (m, 2 H), 3.43−3.75 (m, 3 H), 3.03−3.18 (m, 4 H), 2.12−2.26 (m, 4 H), 1.37 (d, J = 6.9 Hz, 3 H). HRMS: calcd for $C_{44}H_{44}N_7O_8$ [M + H]$^+$ 798.3251; found 798.3260.

Compound 3c. The same procedure as described for the synthesis of **3a** was applied with the exception that the coupling with TCAN/PPh_3 was repeated once to obtain 5.1 mg (58%) of crude product (93% purity as determined by RP-HPLC). RP-HPLC (System B) R_t = 5.30 min. ^{1}H NMR (300 MHz, DMSO-d_6): δ 11.93 (s, 1 H), 10.57 (s, 1 H), 8.78 (d, J = 7.8 Hz, 1 H), 8.62 (d, J = 7.5 Hz, 1 H), 7.99 (d, J = 8.4 Hz, 1 H), 7.55−7.87 (m, 17 H, -NH_3^+ included), 7.25−7.35 (m, 2 H), 7.00−7.22 (m, 4 H), 4.30−4.60 (m, 5 H), 3.40−3.70 (m, overlapped with water peak), 3.05−3.16 (m, 4 H), 2.68−2.77 (m, 2 H), 2.12−2.26 (m, 4 H), 1.85−2.06 (m, 1 H), 1.75 (br), 1.42−1.62 (m, 2 H), 1.27−1.40 (m, 2 H). HRMS: calcd for $C_{47}H_{51}N_8O_8$ [M + H]$^+$ 855.3830; found 855.3853.

Compound 3d. The same procedure as described for the synthesis of **3a** was applied with the exception that the coupling with TCAN/PPh_3 was repeated once to obtain 4.4 mg (56%) crude product (94% purity as determined by RP-HPLC). RP-HPLC (System B) R_t = 8.18 min. ^{1}H NMR (300 MHz, DMSO-d_6): δ 11.95 (s, 1 H), 10.67 (s, 1 H), 8.73 (d, J = 7.8 Hz, 1 H), 8.54 (d, J = 7.5 Hz, 1 H), 7.99 (d, J = 7.5 Hz, 1 H), 7.69−7.93 (m, 12 H, -NH_3^+ included), 7.63 (s, 1 H), 7.54 (t, J = 8.1, 1 H), 7.05−7.35 (m, 6 H), 4.80−4.91 (m, 1 H), 4.47−4.57 (m, 2 H), 4.35−4.45 (m, 2 H), 3.29−3.70 (m, overlapped with water peak), 3.00−3.20 (m, 4 H), 2.81−2.91 (m, 1 H), 2.58−2.71 (m, 1 H), 2.14−2.29 (m, 4 H). HRMS: calcd for $C_{45}H_{44}N_7O_{10}$ [M + H]$^+$ 842.3150; found 842.3165.

Compound 3e. The same procedure as described for the synthesis of **3a** was applied with the exception that the coupling with TCAN/PPh_3 was repeated once to obtain 4.7 mg (58%) of crude product (96% purity as determined by RP-HPLC). RP-HPLC (System C) R_t = 7.18 min. ^{1}H NMR (300 MHz, DMSO-d_6): δ 11.92 (s, 1 H), 10.64 (s, 1 H), 8.80 (d, J = 7.5 Hz, 1 H), 8.62 (d, J = 7.8 Hz, 1 H), 7.99 (d, J = 8.4 Hz, 1 H), 7.70−7.87 (m, 12 H, -NH_3^+ included), 7.55−7.65 (m, 2 H), 7.25−7.35 (m, 2 H), 6.97−7.21 (m, 9 H), 4.65−4.80 (m, 1 H), 4.47−4.57 (m, 2 H), 4.35−4.45 (m, 2 H), 3.50−3.65 (m, 1 H), 2.85−3.20 (m, 5 H), 2.12−2.25 (m, 4 H). HRMS: calcd for $C_{50}H_{48}N_7O_8$ [M + H]$^+$ 874.3564; found 874.3583.

Compound 3f. The same procedure as described for the synthesis of **3a** was applied with the exception that the coupling with TCAN/PPh_3 was repeated three times to obtain 4.0 mg (52%) of crude product (97% purity as determined by RP-HPLC). RP-HPLC (System B) R_t = 8.58 min. ^{1}H NMR (300 MHz, DMSO-d_6): δ 11.78 (s, 1 H), 10.87 (s, 1 H), 8.80 (dd, J = 7.5, 0.9 Hz, 1 H), 8.65 (d, J = 7.5 Hz, 1 H), 7.99 (dd, J = 8.4, 1.2 Hz, 1 H), 7.61−7.91 (m, 13 H, -NH_3^+ included), 7.53 (d, J = 8.1, 1 H), 7.30−7.48 (m, 4 H), 7.15−7.28 (m, 2 H), 4.49−4.59 (m, 3 H), 4.38−4.48 (m, 2 H), 3.65−3.91 (m, overlapped with water peak), 3.01−3.23 (m, 4 H), 2.17−2.29 (m, 4 H). HRMS: calcd for $C_{44}H_{44}N_7O_9$ [M + H]$^+$ 814.3201; found 814.3210.

Compound 3g. The same procedure as described for the synthesis of **3a** was applied with the exception that the coupling with TCAN/PPh_3 was repeated twice to obtain 3.6 mg (46%) of crude product (97% purity as determined by RP-HPLC). RP-HPLC (System B) R_t = 11.33 min. ^{1}H NMR (300 MHz, DMSO-d_6): δ 11.97 (s, 1 H), 10.57 (s, 1 H), 9.32 (br, 1 H), 8.77 (dd, J = 7.8, 1.2 Hz, 1 H), 8.65 (d, J = 7.8 Hz, 1 H), 8.02 (d, J = 7.5, 1 H), 7.62−7.89 (m, 14 H, -NH_3^+ included), 7.28−7.41 (m, 4 H), 7.13−7.22 (m, 2 H), 4.49−4.70 (m, 3 H), 4.37−4.49 (m, 2 H), 3.67−3.82 (m, 1 H), 3.45−3.65 (m, overlapped with water peak), 3.03−3.18 (m, 5 H), 2.84−2.98 (m, 1 H), 2.12−2.26 (m, 4 H). HRMS: calcd for $C_{44}H_{44}N_7O_8S$ [M + H]$^+$ 830.2972; found 830.2985.

Compound 4a. Synthesis started from Wang resin on a 3.8 μmol scale (10 mg resin with manufacturer's loading: 0.38 mmol g^{-1}) to obtain 2.3 mg of crude product. RP-HPLC (System A) R_t = 8.39 min (corresponding to DL byproduct, 2% total peak area), 8.89 min (corresponding to LL product, 98% total peak area). ^{1}H NMR (300 MHz, DMSO-d_6): δ 11.92 (s, 1 H), 10.23 (s, 1 H), 8.79 (d, J = 7.5 Hz, 1 H), 8.72 (d, J = 7.8 Hz, 1 H), 8.19 (d, J = 6.6 Hz, 1 H), 7.93−8.06 (m, 2 H), 7.57−7.89 (m, 14 H, -NH_3^+ included), 7.16−7.46 (m, 5 H), 4.60−4.73 (m, 1 H), 4.36−4.58 (m, 4 H), 4.07−4.16 (m, 2 H), 3.83−3.96 (m, 1 H), 3.50−4.65 (m, overlapped with water peak), 3.03−3.17 (m, 4 H), 2.12−2.26 (m, 4 H), 1.37 (d, J = 6.9 Hz, 3 H), 0.98 (d, J =

DOI: 10.1021/acs.joc.5b02671
J. Org. Chem. 2016, 81, 1137−1150

7.2 Hz, 3 H). HRMS: calcd for $C_{47}H_{49}N_8O_9$ $[M + H]^+$ 869.3617; found 869.3644.

Compound ***4b***. Synthesis started from Wang resin on a 3.8 μmol scale (10 mg resin with manufacturer's loading: 0.38 mmol g^{-1}) to obtain 2.5 mg of crude product. RP-HPLC (System A) R_t = 5.21 min (diastereoisomers could not be separated by RP-HPLC). ^{1}H NMR (300 MHz, DMSO-d_6): δ 11.98 (s, 1 H), 10.22 (s, 1 H), 8.80 (d, *J* = 7.8 Hz, 1 H), 8.69 (d, *J* = 7.5 Hz, 1 H), 8.26 (br, 1 H), 7.95−8.07 (m, 2 H), 7.55−7.89 (m, 20 H, -NH_3^+ included), 7.19−7.46 (m, 5 H), 4.31−4.70 (m, 5 H), 3.68−4.23 (m, 4 H), 3.05−3.16 (m, 4 H), 2.60−2.70 (m, 2 H), 2.50−2.60 (m, overlapped with DMSO peak), 2.07−2.25 (m, 4 H), 1.84−2.06 (m, 1 H), 1.63−1.83 (m, 1 H), 1.16−1.58 (m, 10 H). HRMS: calcd for $C_{53}H_{63}N_{10}O_9$ $[M + H]^+$ 983.4774; found 983,4804.

Compound ***4c***. Synthesis started from Wang resin on a 3.8 μmol scale (10 mg resin with manufacturer's loading: 0.38 mmol g^{-1}) to obtain 2.3 mg of crude product. RP-HPLC (System A) R_t = 7.21 min (corresponding to DL byproduct, 1% total peak area), 7.48 min (corresponding to LL product, 99% total peak area). ^{1}H NMR (300 MHz, DMSO-d_6): δ 12.03 (s, 1 H), 10.42 (s, 1 H), 8.74 (d, *J* = 7.8 Hz, 1 H), 8.68 (d, *J* = 8.1 Hz, 1 H), 8.33 (d, *J* = 7.5 Hz, 1 H), 7.94−8.07 (m, 2 H), 7.47−7.88 (m, 15 H, -NH_3^+ included), 7.21−7.45 (m, 4 H), 4.88−5.11 (m, 1 H), 4.31−4.62 (m, 4 H), 4.01−4.26 (m, 4 H), 3.04−3.18 (m, 4 H), 2.75−2.90 (m, 1 H), 2.50−2.65 (m, overlapped with DMSO peak), 2.15−2.25 (m, 4 H). HRMS: calcd for $C_{49}H_{49}N_8O_{13}$ $[M + H]^+$ 957.3414; found 957.3434.

Compound ***4d***. Synthesis started from Wang resin on a 3.8 μmol scale (10 mg resin with manufacturer's loading: 0.38 mmol g^{-1}) to obtain 2.0 mg of crude product. RP-HPLC (System A) R_t = 13.54 min (corresponding to DL byproduct, 5% total peak area), 14.05 min (corresponding to LL product, 95% total peak area). ^{1}H NMR (300 MHz, DMSO-d_6): δ 11.94 (s, 1 H), 10.20 (s, 1 H), 8.74 (d, *J* = 7.5 Hz, 1 H), 8.69 (d, *J* = 6.9 Hz, 1 H), 8.38 (d, *J* = 7.8 Hz, 1 H), 7.68−7.87 (m, 11 H, -NH_3^+ included), 7.61 (s, 1 H), 7.49−7.56 (m, 2 H), 7.32−7.43 (m, 3 H), 7.18−7.29 (m, 2 H), 6.84−7.11 (m, 10 H), 4.90−5.03 (m, 1 H), 4.34−4.61 (m, 4 H), 3.85−4.23 (m, 3 H), 2.99−3.23 (m, 7 H), 2.76−2.87 (m, 1 H), 2.50−2.65 (m, overlapped with DMSO peak), 2.13−2.25 (m, 4 H). HRMS: calcd for $C_{59}H_{57}N_8O_9$ $[M + H]^+$ 1021.4249; found 1021.4274.

Compound ***4e***. Synthesis started from Wang resin on a 3.8 μmol scale (10 mg resin with manufacturer's loading: 0.38 mmol g^{-1}) to obtain 2.0 mg of crude product. RP-HPLC (System A) R_t = 7.36 min (corresponding to DL byproduct, 2% total peak area), 7.81 min (corresponding to LL product, 98% total peak area). ^{1}H NMR (300 MHz, DMSO-d_6): δ 11.76 (s, 1 H), 10.89 (s, 1 H), 8.69−8.82 (m, 2 H), 8.03 (d, *J* = 8.4 Hz, 1 H), 7.98 (d, *J* = 8.4 Hz, 1 H), 7.86−7.93 (m, 2 H), 7.64−7.85 (m, 13 H, -NH_3^+ included), 7.24−7.46 (m, 5 H), 4.70−4.85 (m, 1 H), 4.43−4.56 (m, 4 H), 4.02−4.30 (m, 4 H), 3.50−3.79 (m, 4 H), 3.07−3.16 (m, 4 H), 2.13−2.26 (m, 4 H). HRMS: calcd for $C_{47}H_{49}N_8O_{11}$ $[M + H]^+$ 901.3515; found 901.3540.

Compound ***5a***. Synthesis started from Wang resin on a 3.8 μmol scale (10 mg resin with manufacturer's loading: 0.38 mmol g^{-1}) to obtain 2.6 mg of crude product. RP-HPLC (System A) R_t = 8.38 min (corresponding to LL product, 99% total peak area), 8.94 min (corresponding to DL byproduct, 1% total peak area). ^{1}H NMR (300 MHz, DMSO-d_6): δ 11.95 (s, 1 H), 10.34 (s, 1 H), 8.78 (d, *J* = 7.8 Hz, 1 H), 8.72 (d, *J* = 7.2 Hz, 1 H), 8.26 (d, *J* = 7.5 Hz, 1 H), 8.02 (d, *J* = 8.4 Hz, 1 H), 7.60−7.97 (m, 14 H, -NH_3^+ included), 7.20−7.59 (m, 6 H), 4.63−4.80 (m, 1 H), 4.37−4.57 (m, 4 H), 3.50−4.10 (m, 4 H), 3.04−3.17 (m, 4 H), 2.12−2.25 (m, 4 H), 1.36 (d, *J* = 6.9 Hz, 3 H), 0.98 (d, *J* = 6.9 Hz, 3 H). HRMS: calcd for $C_{47}H_{49}N_8O_9$ $[M + H]^+$ 869.3617; found 869.3636.

Compound ***5b***. Synthesis started from Wang resin on a 3.8 μmol scale (10 mg resin with manufacturer's loading: 0.38 mmol g^{-1}) to obtain 2.8 mg of crude product. RP-HPLC (System A) R_t = 5.29 min (diastereoisomers could not be separated by RP-HPLC). ^{1}H NMR (300 MHz, DMSO-d_6): δ 11.96 (s, 1 H), 10.34 (s, 1 H), 8.77 (d, *J* = 7.2 Hz, 1 H), 8.69 (d, *J* = 7.8 Hz, 1 H), 8.38 (br, 1 H), 8.03 (d, *J* = 8.4, 1 H), 7.60−7.92 (m, 19 H, -NH_3^+ included), 7.32−7.55 (m, 4 H), 7.18−7.31 (m, 3 H), 4.55−4.71 (m, 1 H), 4.31−4.53 (m, 4 H), 3.64−4.10 (m, 4 H), 3.07−3.16 (m, 4 H), 2.53−2.75 (m, 4 H), 2.13−2.25 (m, 4 H), 1.85−2.06 (m, 1 H), 1.67−1.83 (m, 1 H), 1.16−1.59 (m, 10 H). HRMS: calcd for $C_{53}H_{63}N_{10}O_9$ $[M + H]^+$ 983.4774; found 983,4797.

Compound ***5c***. Synthesis started from Wang resin on a 3.8 μmol scale (10 mg resin with manufacturer's loading: 0.38 mmol g^{-1}) to obtain 1.5 mg of crude product. RP-HPLC (System A) R_t = 7.25 min (corresponding to LL product, 94% total peak area), 7.58 min (corresponding to DL byproduct, 6% total peak area). ^{1}H NMR (300 MHz, DMSO-d_6): δ 12.01 (s, 1 H), 10.46 (s, 1 H), 8.73 (d, *J* = 7.2 Hz, 1 H), 8.68 (d, *J* = 7.8 Hz, 1 H), 8.49 (d, *J* = 7.8 Hz, 1 H), 8.02 (d, *J* = 8.4 Hz, 1 H), 7.63−7.93 (m, 13 H, -NH_3^+ included), 7.48−7.58 (m, 2 H), 7.31−7.46 (m, 3 H), 7.18−7.28 (m, 2 H), 4.92−5.14 (m, 1 H), 4.36−4.59 (m, 4 H), 3.62−4.23 (m, 3 H), 3.35−3.50 (m, overlapped with water peak), 3.06−3.16 (m, 4 H), 2.74−2.95 (m, 1 H), 2.40−2.70 (m, overlapped with DMSO peak), 2.30−2.37 (m, 1 H), 2.10−2.25 (m, 4 H). HRMS: calcd for $C_{49}H_{49}N_8O_{13}$ $[M + H]^+$ 957.3414; found 957.3436.

Compound ***5d***. Synthesis started from Wang resin on a 3.8 μmol scale (10 mg resin with manufacturer's loading: 0.38 mmol g^{-1}) to obtain 2.2 mg of crude product. RP-HPLC (System A) R_t = 13.49 min (corresponding to LL product, 99% total peak area), 14.10 min (corresponding to DL byproduct 1% total peak area). ^{1}H NMR (300 MHz, DMSO-d_6): δ 11.98 (s, 1 H), 10.41 (s, 1 H), 8.75 (d, *J* = 7.8 Hz, 1 H), 8.70 (dd, *J* = 7.5, 0.9 Hz, 1 H), 8.56 (d, *J* = 7.5 Hz, 1 H), 8.01 (dd, *J* = 8.4, 0.9 Hz, 1 H), 7.95 (dd, *J* = 8.4, 0.9 Hz, 1 H), 7.68−7.86 (m, 11 H, -NH_3^+ included), 7.60 (s, 1 H), 7.45−7.54 (m, 2 H), 7.32−7.42 (m, 2 H), 7.16−7.27 (m, 3 H), 6.88−7.16 (m, 10 H), 4.89−5.06 (m, 1 H), 4.34−4.59 (m, 4 H), 3.85−4.16 (m, 3 H), 3.20−3.35 (m, overlapped with water peak), 2.91−3.20 (m, 6 H), 2.28−2.46 (m, 3 H), 2.12−2.25 (m, 4 H). HRMS: calcd for $C_{59}H_{57}N_8O_9$ $[M + H]^+$ 1021.4249; found 1021.4273.

Compound ***5e***. Synthesis started from Wang resin on a 3.8 μmol scale (10 mg resin with manufacturer's loading: 0.38 mmol g^{-1}) to obtain 2.0 mg of crude product. RP-HPLC (System A) R_t = 7.39 min (corresponding to LL product, 98% total peak area), 7.82 min (corresponding to DL byproduct, 2% total peak area). ^{1}H NMR (300 MHz, DMSO-d_6): δ 11.76 (s, 1 H), 10.88 (s, 1 H), 8.67−8.89 (m, 2 H), 7.93−8.08 (m, 2 H), 7.85−7.93 (m, 2 H), 7.63−7.84 (m, 13 H, -NH_3^+ included), 7.35−7.47 (m, 2 H), 7.23−7.35 (m, 3 H), 4.69−4.83 (m, 1 H), 4.44−4.55 (m, 4 H), 4.02−4.28 (m, 4 H), 3.44−3.81 (m, 4 H), 3.07−3.16 (m, 4 H), 2.16−2.26 (m, 4 H). HRMS: calcd for $C_{47}H_{49}N_8O_{11}$ $[M + H]^+$ 901.3515; found 901.3522.

Compound ***7***. To a solution of **6** (2.44 g, 7.5 mmol, 1.5 equiv) in anhydrous DCM under N_2 was added 1-chloro-*N*,*N*,2-trimethyl-1-propenylamine (1.5 mL, 11.25 mmol, 2.25 equiv). The solution was allowed to stir at rt for 2 h. The solvent was then removed on a vacuum manifold (equipped with liquid N_2 solvent trap), and the resulting solid was further dried in this manner for another 3 h to give the corresponding acid chloride (without further purification) in quantitative yield. The resulting acid chloride (2.58 g, 7.5 mmol, 1.5 equiv) in anhydrous THF (30 mL) was added to a solution of methyl 8-amino-4-isobutoxyquinoline-2-carboxylate (1.4 g, 5.0 mmol, 1.0 equiv) in anhydrous THF (30 mL). Anhydrous DIEA (1.3 mL, 7.5 mmol, 1.5 equiv) was added, and the mixture was stirred for 12 h at rt under N_2. The reaction mixture was concentrated and purified by silica gel chromatography (cyclohexane/EtOAc = 1:1) to afford the title compound as a yellow solid (1.75 g, 60%). ^{1}H NMR (300 MHz, $CDCl_3$): δ 10.73 (s, 1H), 8.73 (d, *J* = 7.5 Hz, 1 H), 7.93 (dd, *J* = 8.4, 0.9 Hz, 1 H), 7.71 (br, 2 H), 7.50−7.65 (m, 4 H), 7.15−7.40 (m, overlapped with chloroform peak), 5.92 (br, 1 H), 4.41 (d, *J* = 6.3, 2 H), 4.22 (br, 1 H), 4.06 (d, *J* = 6.3 Hz, 2 H), 3.98 (s, 3 H), 2.22−2.38 (m, 1 H), 1.76 (s, 6 H), 1.15 (d, *J* = 6.9 Hz, 6 H). ^{13}C{^{1}H}NMR (300 MHz, $CDCl_3$): δ 173.07, 165.72, 163.28, 155.23, 146.79, 144.06, 141.38, 139.02, 134.94, 128.50, 127.71, 127.09, 125.21, 122.15, 120.00, 117.66, 115.90, 101.31, 75.39, 66.92, 58.07, 53.03, 47.38, 28.32, 25.69, 19.37. HRMS: calcd for $C_{34}H_{36}N_3O_6$ $[M + H]^+$ 582.2604; found 582.2608.

Compound ***8***. Compound **7** (1.75 g, 3.0 mmol, 1.0 equiv) was dissolved in ethyl acetate (30 mL), and lithium iodide (3.2 g, 24 mmol,

DOI: 10.1021/acs.joc.5b02671
J. Org. Chem. 2016, 81, 1137−1150

8 equiv) was added. The mixture was stirred at reflux for 12 h and then cooled to rt. The mixture was diluted with ethyl acetate (120 mL) and washed with water three times and brine once. The organic layer was dried with Na_2SO_4, filtered, and concentrated under reduced pressure. The crude product was purified by silica gel chromatography (DCM/MeOH = 20:1) to afford the title compound as a yellow solid (1.56 g, 92%). ^{1}H NMR (300 MHz, $CDCl_3$): δ 11.54 (s, 1 H), 8.84 (dd, J = 7.8, 1.2 Hz, 1 H), 7.95 (dd, J = 8.4, 1.2 Hz, 1 H), 7.72 (d, J = 7.5 Hz, 2 H), 7.67 (s, 1 H), 7.53−7.64 (m, 3 H), 7.31 (t, 7.2 Hz, 2 H), 7.20 (td, J = 7.5, 0.9 Hz, 2 H), 5.15 (s, 1 H), 4.64 (d, J = 6.3, 2 H), 4.20 (t, 1 H), 4.08 (d, J = 6.6 Hz, 2 H), 2.22−2.39 (m, 1 H), 1.68 (s, 6 H), 1.14 (d, J = 6.6 Hz, 6 H). ^{13}C{^{1}H}NMR (300 MHz, $CDCl_3$): δ 172.71, 165.60, 163.92, 157.22, 145.99, 143.40, 141.46, 138.05, 135.88, 128.72, 127.83, 127.24, 125.01, 122.67, 120.07, 118.63, 116.11, 99.98, 75.63, 67.33, 58.68, 47.37, 28.26, 25.94, 19.32. HRMS: calcd for $C_{33}H_{34}N_3O_6$ $[M + H]^+$ 568.2448; found 568.2447.

Compound **9**. The title compound was synthesized from dimer block **8** on a 19 μmol scale (50 mg of Wang resin with manufacturer's loading: 0.38 mmol g^{-1}) by using the general SPS methodologies mentioned above and those previously published.[31b] The crude product was purified by silica gel chromatography (DCM/MeOH = 20:1) to afford the title compound as a white solid (16.7 mg, 39%). ^{1}H NMR (300 MHz, $CDCl_3$): δ 12.30 (s, 1 H), 11.78 (s, 1 H), 11.63−11.74 (m, 3 H), 11.58 (s, 1 H), 9.64 (s, 1 H), 9.61 (s, 1 H), 9.50−9.58 (m, 3 H), 8.73−8.93 (m, 7 H), 8.50 (dd, J = 8.4, 1.2 Hz, 1 H), 8.18 (dd, J = 7.2, 1.2 Hz, 1 H), 8.10 (s, 1 H), 7.84−7.99 (m, 6 H), 7.82 (s, 1 H), 7.78 (s, 1 H), 7.75 (s, 1 H), 7.74 (s, 1 H), 7.71 (s, 1 H), 7.47−7.67 (m, 8 H), 4.27 (d, J = 6.3 Hz, 2 H), 4.22 (d, J = 6.0 Hz, 2 H), 4.04−4.16 (m, 8 H), 3.95 (d, J = 5.7 Hz, 2 H), 2.10−2.43 (m, 7 H), 1.94−2.06 (m, 36 H), 1.20 (d, J = 6.6 Hz, 6 H), 1.15 (d, J = 6.6 Hz, 6 H), 1.12 (d, J = 6.6 Hz, 6 H), 1.03−1.10 (m, 18 H), 0.95 (d, J = 6.6 Hz, 6 H). HRMS: calcd for $C_{122}H_{141}N_{20}O_{23}$ $[M + H]^+$ 2255.0512; found 2255.0527.

Compound **10**. The title compound was synthesized on a 19 μmol scale (50 mg of Wang resin with manufacturer's loading: 0.38 mmol g^{-1}) by using the general SPS methodologies mentioned above and those previously published.[31b] The crude product was purified by semipreparative RP-HPLC (System G) to afford the title compound as a white solid (6.9 mg, 15%, purity by RP-HPLC: 97%). RP-HPLC (System E) R_t = 10.20 min. ^{1}H NMR (300 MHz, DMSO-d_6): δ 11.53−11.99 (m, 3 H), 11.43 (s, 1 H), 11.32 (s, 1 H), 10.90 (br, 1 H), 10.32 (br, 2 H), 10.16 (s, 1 H), 10.03 (s, 1 H), 9.07 (s, 1 H), 8.45−8.77 (m, 6 H), 7.73−7.95 (m, 6 H), 7.43−7.65 (m, 11 H), 7.39 (s, 1 H), 6.67 (br), 5.56−5.49 (m, 5 H), 4.48−4.85 (m, 13 H), 2.80−3.10 (m, overlapped with water peak), 2.30−2.70 (m, overlapped with DMSO peak), 1.91−2.15 (m, 1 H), 1.86 (s, 3 H). HRMS: calcd for $C_{98}H_{84}N_{18}O_{44}$ $[M + 2H]^{2+}$ 1108.7461; found 1108.7501.

Compound **11**. The title compound was synthesized on a 19 μmol scale (50 mg of Wang resin with manufacturer's loading: 0.38 mmol g^{-1}) by using the general SPS methodologies mentioned above and those previously published.[31b] The crude product was purified by semipreparative RP-HPLC (System F) to afford the title compound as a yellow solid (13.3 mg, 19%, purity by RP-HPLC: 98%). RP-HPLC (System D) R_t = 7.23 min. ^{1}H NMR (300 MHz, CD_3OH): δ 10.99 (s, 1 H), 10.93 (s, 1 H), 10.05−10.48 (m, 3 H), 10.06−10.22 (m, 2 H), 9.95 (s, 1 H), 9.33−9.58 (m, 2 H), 9.11 (s, 1 H), 8.74−8.95 (m, 2 H), 6.55−8.65 (m, 53 H, -NH_3^+ included), 6.25−6.49 (s, 1 H), 6.11 (s, 1 H), 5.82 (s, 1 H), 3.68−4.55 (m, 4 H), 2.70−3.60 (m, overlapped with CH_3OH peak), 2.00−2.68 (m, 31 H), 1.23−1.92 (m, 39 H). HRMS: calcd for $C_{130}H_{160}N_{32}O_{22}$ $[M+4H]^{4+}$ 630.5605; found 630.5629.

Compound **12**. The title compound was synthesized on a 19 μmol scale (50 mg of Wang resin with manufacturer's loading: 0.38 mmol g^{-1}) by using the general SPS methodologies mentioned above and those previously published.[31b] The crude product was purified by semipreparative RP-HPLC (System F) to afford the title compound as a pale yellow solid (14.4 mg, 23%, purity by RP-HPLC: 98%). RP-HPLC (System D) R_t = 12.77 min. ^{1}H NMR (800 MHz, 10%D_2O/H_2O v/v %): δ 11.10 (br, 1 H), 10.61 (s, 1 H), 10.44 (br, 1 H), 10.28−10.38 (m, 2 H), 10.23 (s, 1 H), 10.05 (s, 1 H), 9.94 (s, 1 H), 9.72 (s, 1 H), 9.44 (s, 1 H), 9.02 (br, 1 H), 8.73 (d, J = 8.0 Hz, 1 H), 8.59 (d, J = 8.0 Hz, 1 H), 8.44 (s, 1 H), 7.00−8.24 (m, 41 H, -NH_3^+ included), 6.70 (d, J = 8.8 Hz, 1 H), 6.81 (d, J = 8.0 Hz, 1 H), 6.67 (t, J = 8.0 Hz, 1 H), 6.61 (s, 1 H), 6.21 (s, 1 H), 5.70 (s, 1 H), 4.60−5.20 (m, overlapped with water peak), 3.74−4.59 (m, 11 H), 3.54−3.67 (m, 4 H), 3.27−3.49 (m, 17 H), 3.19−3.24 (m, 2 H), 2.91−3.03 (m, 2 H), 2.68 (br, 1 H), 2.33−2.56 (m, 19 H), 1.99−2.25 (m, 4 H), 1.69 (br, 1 H), 1.40−1.55 (m, 5 H). HRMS: calcd for $C_{122}H_{138}N_{29}O_{25}$ $[M + 3H]^{3+}$ 803.3484; found 803.3515.

Preparative RP-HPLC (System F) was used to afford the title compound as a yellow solid (13.3 mg, 19%, purity by RP-HPLC: 98%). RP-HPLC (System D) R_t = 7.23 min. ^{1}H NMR (300 MHz, CD_3OH): δ 10.99 (s, 1 H), 10.93 (s, 1 H), 10.05−10.48 (m, 3 H), 10.06−10.22 (m, 2 H), 9.95 (s, 1 H), 9.33−9.58 (m, 2 H), 9.11 (s, 1 H), 8.74−8.95 (m, 2 H), 6.55−8.65 (m, 53 H, -NH_3^+ included), 6.25−6.49 (s, 1 H), 6.11 (s, 1 H), 5.82 (s, 1 H), 3.68−4.55 (m, 4 H), 2.70−3.60 (m, overlapped with CH_3OH peak), 2.00−2.68 (m, 31 H), 1.23−1.92 (m, 39 H). HRMS: calcd for $C_{130}H_{160}N_{32}O_{22}$ $[M + 4H]^{4+}$ 630.5605; found 630.5661.

Compound **12**. The title compound was synthesized on a 19 μmol scale (50 mg of Wang resin with manufacturer's loading: 0.38 mmol g^{-1}) by using the general SPS methodologies mentioned above and those previously published.[31b] The crude product was purified by semipreparative RP-HPLC (System F) to afford the title compound as a pale yellow solid (14.4 mg, 23%, purity by RP-HPLC: 98%). RP-HPLC (System D) R_t = 12.77 min. ^{1}H NMR (800 MHz, 10% D_2O/H_2O v/v %): δ 11.10 (br, 1 H), 10.61 (s, 1 H), 10.44 (br, 1 H), 10.28−10.38 (m, 2 H), 10.23 (s, 1 H), 10.05 (s, 1 H), 9.94 (s, 1 H), 9.72 (s, 1 H), 9.44 (s, 1 H), 9.02 (br, 1 H), 8.73 (d, J = 8.0 Hz, 1 H), 8.59 (d, J = 8.0 Hz, 1 H), 8.44 (s, 1 H), 7.00−8.24 (m, 41 H, -NH_3^+ included), 6.70 (d, J = 8.8 Hz, 1 H), 6.81 (d, J = 8.0 Hz, 1 H), 6.67 (t, J = 8.0 Hz, 1 H), 6.61 (s, 1 H), 6.21 (s, 1 H), 5.70 (s, 1 H), 4.60−5.20 (m, overlapped with water peak), 3.74−4.59 (m, 11 H), 3.54−3.67 (m, 4 H), 3.27−3.49 (m, 17 H), 3.19−3.24 (m, 2 H), 2.91−3.03 (m, 2 H), 2.68 (br, 1 H), 2.33−2.56 (m, 19 H), 1.99−2.25 (m, 4 H), 1.69 (br, 1 H), 1.40−1.55 (m, 5 H). HRMS: calcd for $C_{122}H_{138}N_{29}O_{25}$ $[M + 3H]^{3+}$ 803.3484; found 803.3515.

NMR Spectroscopy. Spectra were recorded on four different NMR spectrometers: (1) a Bruker Avance II NMR spectrometer operating at 300 MHz for ^{1}H observation and 75 MHz for ^{13}C observation by means of a 5 mm direct BBO H/X probe with Z gradient capabilities; (2) a Bruker Avance DPX spectrometer operating at 400 MHz for correlation spectroscopy (COSY) experiment by means of a 5 mm QNP ^{1}H/^{13}C/^{19}F/^{31}P/^{2}H probe with Z gradient capabilities; (3) a Bruker Avance III spectrometer operating at 700 MHz for total correlation spectroscopy (TOCSY), heteronuclear single quantum coherence (HSQC), heteronuclear multiple bond correlation (HMBC) and rotating-frame overhauser effect spectroscopy (ROESY) experiments by means of a 5 mm TXI ^{1}H/^{13}C/^{15}N/^{2}H probe with Z gradient capabilities; and (4) a Bruker Avance III spectrometer operating at 800 MHz for nuclear overhauser effect spectroscopy (NOESY) experiments by means of a 5 mm TCI ^{1}H/^{13}C/^{15}N/^{2}H probe with Z gradient capabilities. Data processing was performed with Topspin software. COSY acquisition was performed with a time domain size of 2048 (F2) × 256 (F1), 48 scans per increment, a pulse program of cosydfgpph19, and water suppression using 3-9-19 pulse sequence. TOCSY acquisition was performed with a time domain size of 2048 (F2) × 128 (F1), 80 scans per increment, a pulse program of dipsi2esgpph, a mixing time of 150 ms, and water suppression using excitation sculpting. HSQC acquisition was performed with a time domain size of 2048 (F2) × 131 (F1), 128 scans per increment, and a pulse program of hsqcedetgp. HMBC acquisition was performed with a time domain size of 2048 (F2) × 128 (F1), 128 scans per increment, a pulse program of hmbcgplpndprqf, a coupling constant of 7 Hz, and water suppression using presaturation. NOESY acquisition was performed with a time domain size of 2048 (F2) × 475 (F1), 64 scans per increment, a pulse program of noesyesgpph, a mixing time of 300 ms, and water suppression using excitation sculpting. ROESY acquisition was performed with a time domain size of 2048 (F2) × 128 (F1), 128

DOI: 10.1021/acs.joc.5b02671
J. Org. Chem. 2016, 81, 1137−1150

scans per increment, a pulse program of roesyesgpph, a mixing time of 200 ms, and water suppression using excitation sculpting.

Molecular Modeling. MacroModel version 8.6 (Schrödinger Inc.) was used for building all of the molecular models. The minimization conditions: force field, MMFFs; solvent, none; cutoff, extended; method, TNCG; and maximum iterations, 500) are constant throughout the calculations. To begin, an ill-folded structure of **12** with a left-handed or right-handed helical twist was employed to perform energy minimization by importing the distances information calculated from the selected NOE data (see Supporting Information) as the constrained distances. After trying several different starting points, all of the ill-folded structures with a left-handed twist failed to generate any uniform conformation (each time giving a different irregular conformation) after energy minimization. In contrast, the ill-folded structures with a right-handed twist formed a helical structure, which was consistent with CD data. With the first molecular model in hand, another 19 molecular models were obtained to estimate their stability. To access the following 19 molecular models, the first molecular model was randomly released to an ill-folded structure again. Then, energy minimization was carried out via the same method to afford the second molecular model. This process was repeated 18 times to obtain all 20 molecular models. Root-mean-square deviation data was generated in PyMOL.

■ ASSOCIATED CONTENT

Supporting Information

The Supporting Information is available free of charge on the ACS Publications website at DOI: 10.1021/acs.joc.5b02671.

Racemization assessment supported by RP-HPLC and ^{1}H NMR, CD and ^{1}H NMR investigations, detailed 2D NMR structural investigation, molecular modeling, and characterization data of new compounds (PDF)

■ AUTHOR INFORMATION

Corresponding Author

*E-mail: i.huc@iecb.u-bordeaux.fr.

Notes

The authors declare no competing financial interest.

■ ACKNOWLEDGMENTS

The authors would like to thank Dr. Mohamed Elsawy for assistance in preliminary work exploring SPS conditions. This work was supported by the China Scholarship Council (PhD scholarship to X.H.) and the European Research Council (Grant Agreement Number ERC-2012-AdG-320892, postdoctoral fellowship to S.D.).

■ REFERENCES

(1) (a) Gething, M. J.; Sambrook, J. *Nature* **1992**, *355*, 33−45. (b) Nicholls, A.; Sharp, K. A.; Honig, B. *Proteins: Struct., Funct., Genet.* **1991**, *11*, 281−296.

(2) Jones, S.; Thornton, J. M. *Proc. Natl. Acad. Sci. U. S. A.* **1996**, *93*, 13−20.

(3) (a) Xiong, J. P.; Stehle, T.; Zhang, R.; Joachimiak, A.; Frech, M.; Goodman, S. L.; Arnaout, M. A. *Science* **2002**, *296*, 151−155. (b) Wilchek, M.; Bayer, E. A.; Livnah, O. *Immunol. Lett.* **2006**, *103*, 27−32.

(4) (a) Benkovic, S. J.; Hammes-Schiffer, S. *Science* **2003**, *301*, 1196−1202. (b) Russell, A. J.; Fersht, A. R. *Nature* **1987**, *328*, 496−500.

(5) Syed, R. S.; Reid, S. W.; Li, C.; Cheetham, J. C.; Aoki, K. H.; Liu, B.; Zhan, H.; Osslund, T. D.; Chirino, A. J.; Zhang, J.; Finer-Moore, J.; Elliott, S.; Sitney, K.; Katz, B. A.; Matthews, D. J.; Wendoloski, J. J.; Egrie, J.; Stroud, R. M. *Nature* **1998**, *395*, 511−516.

(6) (a) Luecke, H.; Quiocho, F. A. *Nature* **1990**, *347*, 402−406. (b) Nagle, L. F.; Morowitz, H. J. *Proc. Natl. Acad. Sci. U. S. A.* **1978**, *75*, 298−302.

(7) (a) Hintermann, T.; Gademann, K.; Jaun, B.; Seebach, D. *Helv. Chim. Acta* **1998**, *81*, 983−1002. (b) Vila, J. A.; Ripoll, D. R.; Scheraga, H. A. *Proc. Natl. Acad. Sci. U. S. A.* **2000**, *97*, 13075−13079. (c) Frackenpohl, J.; Arvidsson, P. I.; Schreiber, J. V.; Seebach, D. *ChemBioChem* **2001**, *2*, 445−455.

(8) (a) DeGrado, W. F.; Schneider, J. P.; Hamuro, Y. *J. Pept. Res.* **1999**, *54*, 206−217. (b) Gellman, S. H. *Acc. Chem. Res.* **1998**, *31*, 173−180. (c) Seebach, D.; Matthews, J. L. *Chem. Commun.* **1997**, 2015−2022. (d) Baldauf, C.; Gunther, R.; Hofmann, H. J. *J. Org. Chem.* **2006**, *71*, 1200−1208. (e) Baldauf, C.; Gunther, R.; Hofmann, H. J. *J. Org. Chem.* **2004**, *69*, 6214−6220. (f) Hintermann, T.; Gademann, K.; Jaun, B.; Seebach, D. *Helv. Chim. Acta* **1998**, *81*, 983−1002. (g) Hanessian, S.; Luo, X.; Schaum, R.; Michnick, S. *J. Am. Chem. Soc.* **1998**, *120*, 8569−8570.

(9) (a) Baldwin, R. L.; Rose, G. D. *Trends Biochem. Sci.* **1999**, *24*, 26−33. (b) Lyu, P. C.; Sherman, J. C.; Chen, A.; Kallenbach, N. R. *Proc. Natl. Acad. Sci. U. S. A.* **1991**, *88*, 5317−5320.

(10) (a) Sanborn, T. J.; Wu, C. W.; Zuckermann, R. N.; Barron, A. E. *Biopolymers* **2002**, *63*, 12−20. (b) Wu, C. W.; Sanborn, T. J.; Huang, K.; Zuckermann, R. N.; Barron, A. E. *J. Am. Chem. Soc.* **2001**, *123*, 6778−6784.

(11) Burgess, K.; Linthicum, K. S.; Shin, H. *Angew. Chem., Int. Ed. Engl.* **1995**, *34*, 907−909.

(12) Kim, Y. W.; Grossmann, T. N.; Verdine, G. L. *Nat. Protoc.* **2011**, *6*, 761−771.

(13) (a) Hill, D. J.; Mio, M. J.; Prince, R. B.; Hughes, T. S.; Moore, J. S. *Chem. Rev.* **2001**, *101*, 3893−4011. (b) Guichard, G.; Huc, I. *Chem. Commun.* **2011**, *47*, 5933−5941.

(14) Orner, B. P.; Ernst, J. T.; Hamilton, A. D. *J. Am. Chem. Soc.* **2001**, *123*, 5382−5383.

(15) Saraogi, I.; Hamilton, A. D. *Biochem. Soc. Trans.* **2008**, *36*, 1414−1417.

(16) Rodriguez, J. M.; Nevola, L.; Ross, N. T.; Lee, J. I.; Hamilton, A. D. *ChemBioChem* **2009**, *10*, 829−833.

(17) Cummings, C. G.; Hamilton, A. D. *Curr. Opin. Chem. Biol.* **2010**, *14*, 341−346.

(18) (a) Plante, J. P.; Burnley, T.; Malkova, B.; Webb, M. E.; Warriner, S. L.; Edwards, T. A.; Wilson, A. J. *Chem. Commun.* **2009**, 5091−5093. (b) Wilson, A. J. *Chem. Soc. Rev.* **2009**, *38*, 3289−3300. (c) Barnard, A.; Long, K.; Martin, H. L.; Miles, J. A.; Edwards, T. A.; Tomlinson, D. C.; Macdonald, A.; Wilson, A. J. *Angew. Chem.* **2015**, *127*, 3003−3008. (d) Azzarito, V.; Miles, J. A.; Fisher, J.; Edwards, T. A.; Warriner, S. L.; Wilson, A. J. *Chem. Sci.* **2015**, *6*, 2434−2443.

(19) (a) Volonterio, A.; Moisan, L.; Rebek, J., Jr. *Org. Lett.* **2007**, *9*, 3733−3736. (b) Moisan, L.; Odermatt, S.; Gombosuren, N.; Carella, A.; Rebek, J., Jr. *Eur. J. Org. Chem.* **2008**, *2008*, 1673−1676.

(20) Maity, P.; Konig, B. *Org. Lett.* **2008**, *10*, 1473−1476.

(21) Xin, D.; Perez, L. M.; Ioerger, T. R.; Burgess, K. *Angew. Chem., Int. Ed.* **2014**, *53*, 3594−3598.

(22) Gillies, E. R.; Deiss, F.; Staedel, C.; Schmitter, J. M.; Huc, I. *Angew. Chem., Int. Ed.* **2007**, *46*, 4081−4084.

(23) Qi, T.; Maurizot, V.; Noguchi, H.; Charoenraks, T.; Kauffmann, B.; Takafuji, M.; Ihara, H.; Huc, I. *Chem. Commun.* **2012**, *48*, 6337−6339.

(24) Delsuc, N.; Kawanami, T.; Lefeuvre, J.; Shundo, A.; Ihara, H.; Takafuji, M.; Huc, I. *ChemPhysChem* **2008**, *9*, 1882−1890.

(25) (a) Jiang, H.; Léger, J.-M.; Huc, I. *J. Am. Chem. Soc.* **2003**, *125*, 3448−3449. (b) Dolain, C.; Grélard, A.; Laguerre, M.; Jiang, H.; Maurizot, V.; Huc, I. *Chem. - Eur. J.* **2005**, *11*, 6135−6144.

(26) Iriondo-Alberdi, J.; Laxmi-Reddy, K.; Bouguerne, B.; Staedel, C.; Huc, I. *ChemBioChem* **2010**, *11*, 1679−1685.

(27) Muller, S.; Laxmi-Reddy, K.; Jena, P. V.; Baptiste, B.; Dong, Z.; Godde, F.; Ha, T.; Rodriguez, R.; Balasubramanian, S.; Huc, I. *ChemBioChem* **2014**, *15*, 2563−2570.

DOI: 10.1021/acs.joc.5b02671
J. Org. Chem. 2016, 81, 1137−1150

(28) Buratto, J.; Colombo, C.; Stupfel, M.; Dawson, S. J.; Dolain, C.; d'Estaintot, B. L.; Fischer, L.; Granier, T.; Laguerre, M.; Gallois, B.; Huc, I. *Angew. Chem., Int. Ed.* **2014**, *53*, 883−887.
(29) Nair, R. V.; Vijayadas, K. N.; Roy, A.; Sanjayan, G. J. *Eur. J. Org. Chem.* **2014**, *2014*, 7763−7780.
(30) Kudo, M.; Maurizot, V.; Kauffmann, B.; Tanatani, A.; Huc, I. *J. Am. Chem. Soc.* **2013**, *135*, 9628−9631.
(31) (a) Sánchez-García, D.; Kauffmann, B.; Kawanami, T.; Ihara, H.; Takafuji, M.; Delville, M.-H.; Huc, I. *J. Am. Chem. Soc.* **2009**, *131*, 8642−8648. (b) Baptiste, B.; Douat-Casassus, C.; Laxmi-Reddy, K.; Godde, F.; Huc, I. *J. Org. Chem.* **2010**, *75*, 7175−7185.
(32) (a) Prabhakaran, P.; Kale, S. S.; Puranik, V. G.; Rajamohanan, P. R.; Chetina, O.; Howard, J. A.; Hofmann, H. J.; Sanjayan, G. J. *J. Am. Chem. Soc.* **2008**, *130*, 17743−17754. (b) Srinivas, D.; Gonnade, R.; Ravindranathan, S.; Sanjayan, G. J. *J. Org. Chem.* **2007**, *72*, 7022−7025. (c) Roy, A.; Prabhakaran, P.; Baruah, P. K.; Sanjayan, G. J. *Chem. Commun.* **2011**, *47*, 11593−11611. (d) Kudo, M.; Maurizot, V.; Masu, H.; Tanatani, A.; Huc, I. *Chem. Commun.* **2014**, *50*, 10090−10093.
(33) (a) Carpino, L. A.; Beyermann, M.; Wenschuh, H.; Bienert, M. *Acc. Chem. Res.* **1996**, *29*, 268−274. (b) Bodanszky, M. *Principles of Peptide Synthesis*. Springer-Verlag: Berlin, 1984. (c) Falb, E.; Yechezkel, T.; Salitra, Y.; Gilon, C. *J. Pept. Res.* **1999**, *53*, 507−517.
(34) Carpino, L. A. *J. Am. Chem. Soc.* **1993**, *115*, 4397−4398.
(35) Frerot, E.; Coste, J.; Pantaloni, A.; Dufour, M. N.; Jouin, P. *Tetrahedron* **1991**, *47*, 259−270.
(36) Waghmare, A. A.; Hindupur, R. M.; Pati, H. N. *Review Journal of Chemistry* **2014**, *4*, 53−131.
(37) Kunishima, M.; Kawachi, C.; Monta, J.; Terao, K.; Iwasaki, F.; Tani, S. *Tetrahedron* **1999**, *55*, 13159−13170.
(38) Jang, D. O.; Park, D. J.; Kim, J. *Tetrahedron Lett.* **1999**, *40*, 5323−5326.
(39) Vágó, I.; Greiner, I. *Tetrahedron Lett.* **2002**, *43*, 6039−6041.
(40) Rich, D. H.; Singh, J. *The peptides*. Academic Press: New York, 1979.
(41) Baptiste, B.; Zhu, J.; Haldar, D.; Kauffmann, B.; Léger, J. M.; Huc, I. *Chem. - Asian J.* **2010**, *5*, 1364−1375.
(42) Dawson, S. J.; Mészáros, Á.; Pethő, L.; Colombo, C.; Csékei, M.; Kotschy, A.; Huc, I. *Eur. J. Org. Chem.* **2014**, *2014*, 4265−4275.
(43) Ammalahti, E.; Bardet, M.; Molko, D.; Cadet, J. *J. Magn. Reson., Ser. A* **1996**, *122*, 230−232.
(44) Qi, T.; Deschrijver, T.; Huc, I. *Nat. Protoc.* **2013**, *8*, 693−708.

DOI: 10.1021/acs.joc.5b02671
J. Org. Chem. 2016, 81, 1137−1150